REAL-TIME PROCESSING OF PHYSIOLOGICAL SIGNALS FOR FEEDBACK CONTROL

A Thesis Submitted to the College of

Graduate Studies and Research

In Partial Fulfillment of the Requirements

For the Degree of Master of Science

In the Division of Biomedical Engineering

University of Saskatchewan

Saskatoon

By

JAYDRATH D BUTALA

Permission to Use

In presenting this thesis in partial fulfilment of the requirements for a Postgraduate degree from the University of Saskatchewan, I agree that the Libraries of this University may make it freely available for inspection. I further agree that permission for copying of this thesis in any manner, in whole or in part, for scholarly purposes may be granted by the professor or professors who supervised my thesis work or, in their absence, by the Head of the Department or the Dean of the College in which my thesis work was done. It is understood that any copying or publication or use of this thesis or parts thereof for financial gain shall not be allowed without my written permission. It is also understood that due recognition shall be given to me and to the University of Saskatchewan in any scholarly use which may be made of any material in my thesis.

Requests for permission to copy or to make other use of material in this thesis in whole or part should be addressed to:

Head of the Division of Biomedical Engineering

University of Saskatchewan

Saskatoon, Saskatchewan (S7N5A9)

ABSTRACT

Extensive studies about neural mechanisms involved in insect flight control have been carried out. Adaptive control of locomotion requires integration of salient sensory cues with ongoing motor activity. During flight, inputs received by an organism through sensory organs are processed by the central nervous system (CNS) and the integrated output thus obtained plays a significant role in controlling the wing phase shifts and flight muscle depressor asymmetries associated with adaptive flight maneuvers. The resulting maneuvers, in turn, bring a change in the insect's sensory environment, thereby closing the feedback loop. Research on insect flight has been carried out using immobile preparations (tethered) and mobile preparations (free flight – untethered). There are pros and cons associated with the tethered and the untethered approach. The tethered approach, however, provides an easier way to study the CNS and its role in motor control of flight. Insects such as locusts and moths exhibit pertinent wing phase shifts and asymmetries in depressor muscles. For locusts constant wing phase shifts and m97 (forewing first basalar depressor muscle) depressor asymmetries have been observed during adaptive flight maneuvers making this a useful system for creation of behaviorally appropriate visual feedback. A method that utilizes asymmetrical timing of bilateral depressor muscles, the forewing first basalars (m97), of the locust to close a visual feedback loop in a computer-generated flight simulator is presented here. The method converts the time difference between left and right m97s to analog voltage values. Analog voltage values can be acquired using an open-loop experimental protocol (visual motion

controlled by the experimenter), or can be used to control closed-loop experiments (muscle activity controls the visual stimuli) experiments. We recorded electromyographic (EMG) activity from right and left m97 muscles. On testing this circuit with real animals, we were able to detect the spike time difference and convert it to voltage values. These voltage values were utilized to control the presentation of a stimulus in a closed-loop environment. The feedback circuit presented here may be used in conjunction with the flight simulator(s) to understand the neural mechanisms involved in control of insect flight and provide further understanding of general mechanisms of neural control of behaviour.

ACKNOWLEDGMENTS

I appreciate the help and support I received from numerous individuals to complete this thesis work. First, I thank my supervisors for providing valuable feedback and suggestions in completion of this thesis work. I really appreciate the technical support I received from Dr. Victor Rush and his team at Tucker Davis Technologies Ltd. Florida, USA. I would like to express my sincere gratitude to the Dept. of Mathematics & Statistics and the Math Help Center, Univ. of Saskatchewan for hiring me as teaching assistant and helping me to fund my research work.

I would like to convey special thanks to my friends Tony Arkles and Dr. Julio Blas, for helping me with my research and thesis work. I also thank my friends Robin Kusch and Graham Fairhurst for providing feedback on my thesis work.

I could not have done this without the support of my family, especially my grandmother Kapila Butala, my parents Dinesh and Aruna, my aunt Pragna, and my brother Sughosh. I also acknowledge the support I have received from my lovely friends Amy Hutton, Jessica Stolar, Erika Quiring, Nina Mohr, Christopher Borsa and many other individuals in this mortal world.

TABLE OF CONTENTS

Page

LIST OF FIGURES

LIST OF APPENDIX FIGURES

LIST OF ABBREVIATIONS

A/D Analog to Digital Converter

D/A Digital to Analog Convertor

DA Depressor Asymmetry

DSP Digital Signal Proccesor

EMG Electromyogram

FWA Forewing Asymmetries

I/O Input/output

LGMD Lobula Giant Movement Detector neuron

RP Real-time Processor

SHARC ® Super Harvard Architecture

TDT Tucker Davis Technologies Ltd.

TTL Transistor-transistor logic

UAV Unmanned Aerial Vehicle

List of Software Terminology [38]

AND - a logical AND gate

'ButCoef1' - component used to generate filter coefficients for second order butterworth filters

'Circuit' - a block diagram representation of a design in the 'RPvdsEx' software performing specific tasks allocated to the DSP saved as pages.

'CycUsage' - component determing the processing power as a function of the tasks alloted to the digital signal processor (based on a scale of 100).

'CompTo16D' - a data compression component used in 'RPvdsEx'

'data tank' - a data storage protocol in the software similar to a file and folder

'diff' - Depressor asymmetry time difference in software

'EA' - tag (root) associated with circuit header 'OxSnippet'

'cEA~1' - parameter tag used to communicate with 'SortSpike2' component of channel 1

'cEA~2' - parameter tag used to communicate with 'SortSpike2' component of channel 2

'FakeSel~1’ - a parameter tag used with multiplexer components

'FakeSel~2' - a parameter tag used with multiplexer components

'FindFreq' - Frequency detecting component

'HopTo' and 'HopFrom' - parameter componets used in pairs to enable graphical breaks in the circuit design [3]. For feedback control circuit, 'HopTo' and 'HopFrom' carry the output of 'Strobe ' component making it accessible between various DSPs.

'iTime' - a component designed to assign time stamp

'Latch' - used to latch (assign) time stamp value via 'iTime' to 'Trig1.' and 'Trig2.'

'MuxIn' - represents a multiplexer in the software for acquiring multiple signals and permitts to have a user defined signal as output

'OpenBrowser' - part of software suite for using System 3

'OpenController' - part of software suite for using System 3

'OpenEx' - Software suite provided by Tucker Davis Technologies Ltd. for controlling the experiments in real-time using a client-server platform [3]

'OpenScope' - part of software suite for using System 3

'OpenWorkbench' - part of software suite for using System 3

OR - a logical OR gate

'OxSnippet' - circuit headers required in the 'RPvdsEx' software to communicate with 'OpenEx' when performing spike detection/sorting operations [3]

'OxStream' - circuit headers required in the 'RPvdsEx' software to communicate with 'OpenEx' when continuous waveforms are acquired [3]

Parameter tags - components used to control various component variables in real-time via 'OpenEx' or other softwares [3]

'PD' - tag (root) associated with circuit header 'OxStream'

'dPD~1' - parameter tags associated with PlotDec16 component for channel 1

'dPD~2' - parameter tags associated with PlotDec16 component for channel 2

'PlotDec16' - a data reduction component used in 'RPvdsEx'

'RAW' - tag (root) associated with circuit header 'OxStream' when used for data compression

'dRAW~1' - parameter tag to indicate data storage for channel 1 when used with 'CompTo16D'

'dRAW~2' - parameter tag to indicate data storage for channel 2 when used with 'CompTo16D'

dRAW~3' - parameter tag to indicate data storage for channel 3 when used with 'CompTo16D' to store data using RP2.1 processors

'sRAW' - a parameter tag to indicate the current position of the buffer

'RawSig1' - a parameter tag for unfiltered signal from channel l

'RawSig2 '- a parameter tag for unfiltered signal from channel 2

RP2.1 Real-Time Processor - based on single DSP architecture [3]

'RPvdsEx' - RP Visual DesignStudio - used to design circuits [3]

'RX5 Pentusa base station' - data acquisition system comprising of multiple Digital Signal processors provided by Tucker Davis Technologies Ltd. Florida, USA

'ScaleAdd' - component in the software used to perform basic mathematical operations for two or more signals

'SerStore' - a write only buffer

SHARC ® - Southern Harvard Architecture

'SIG1_FILT' - filtered EMG signal from channel 1

'SIG2_FILT' - filtered EMG signal from channel 2

'sliders' - a visualizaton control available in 'OpenController' to control filter cut-off frequencies, signal channels, etc.

'SimpCount' - a counter desinged in the 'RPvdsEx' software

'SortSpike2' - SpikeSorting / Spike detecting component

'Spk_FREQ.HPFreq' - 'slider' in 'OpenController' for controlling cut-off frequency of high pass filter in real-time

'Spk_FREQ.LPFreq' - 'slider' in 'OpenController' for controlling cut-off frequency of low pass filter in real-time

'Strobe' - a feature of the 'SortSpike2' component producing logical high signal with detection of every spike

'SwNum'- a parameter tag

'zSwCount' - a parameter tag pertaining to sweep construct

'zSwDone ' a parameter tag

'zSwPeriod' - a parameter tag pertaining to sweep construct

System 3 - Data-acquistion system comprising of RX 5 and RP 2.1 processors provided by Tucker Davis Technlogies Ltd. Florida, USA

'T1' - floating point time stamp values obtained from channel 1

'T2' - floating point time stamp values obtained from channel 2

Tag root - suffix to identify a specific parameter tag associated with various circuit constructs

'Trig. 1' - a logical high signal produced when spike on channel 1 is detected

'Trig. 2' - a logical high signal produced when spike on channel 2 is detected

'TTL2Float' - converts Transistor Transistor Logic values to floating point values

'UseSign' - a feature of the 'SortSpike2' component

CHAPTER 1

INTRODUCTION

Control of complex tasks for both animals and humans require two-way information exchanges. The sense organs receive the information and feed it to brain and from the brain it is fed back to the motor system. This motor system responsible for movement execution requires a feedback loop (common examples: auditory and/or visual feedback) for reliable movement execution. Motor planning, control and adaptation rely on feedback. A feedback loop compensating for errors is necessary to have a robust performance of an interface between brain and computer/machine, and neural prosthetic systems, which are being controlled in real-time. Without a feedback loop tasks like walking, running, and flying will result in an unstable system.

Various animal and insect model systems have been used in an attempt to understand the neural mechanisms that underlie adaptive behavior. For insects, these adaptive behaviors are exhibited during flight in the real world, encountering unpredictable situations, such as avoiding a sudden attack by a predator or an obstacle in its path. The relationships between visual neurons and flight torque [1], visual interneuron activity [2], collision avoidance [3,4] and flight steering [5,6,7] have been the subject of study. The results of these studies suggest that a high level of integration of sensory input, its processing and feedback in accordance with motor control exists in the insect world. Since most of the motor activity is regulated by the insect sensory system, re-engineering these mechanisms in robot hardware and software may provide useful insights into these highly evolved natural sensory networks.

Much research has focused on stimulus detection and perception, sensory motor integration and motor output contributing to the establishment of a well characterized set of flight behaviors. Studies involving insects such as moths [8], locusts [2,5,6,9,10,11,12,13,14,15,16,17,18,19] and flies [1,20,21,22,23,24,25] have been carried out to

understand the flight motor pattern and prevailing sensory input that play a role in flight pattern. Flight simulators have been used to investigate behavioral responses of neurons to visual stimuli. A flight simulator combining a realistic and interactive visual environment with mechanosensory and olfactory stimuli has been effective in addressing questions of insect flight and has also provided the ability to perform experiments in open-loop and closed-loop conditions [26].

Open-loop and closed-loop experiments deal with tethered and non-tethered insect flight. Visual environments provided to the insect in an open-loop experiment are controlled by the experimenter and not modified by the animal's behavioral response [26]. The closed-loop experiment protocol employed by Gray et al. [26] focuses on detection of the insect's abdomen using a photodiode sensor (optical approach) and using the sensor's voltage output to control the movement of the visual environment. The work presented here describes a new methodology to study flight control in insects utilizing electromyogram (EMG) signals obtained from the depressor muscles of locust wings. The occurrence of an action potential, indicating firing of a motor neuron in m97 (right and left forewing first basalar depressor) muscles, has been considered as a good indicator for steering movements in locust flight [27]. During turning maneuvers, asymmetries are observed in the timing of firing of motor neurons in the right and left forewing first basalar (m97) depressor muscles of the locusts [28]. The method presented here utilizes this asymmetrical timing of bilateral depressor muscles, the forewing first basalars (m97), and wing beat frequency of the locust to close a visual feedback loop in a computer-generated flight simulator.

The method converts the wing beat frequency and the depressor asymmetry (DA) time difference to analog voltage values V1 and V2 respectively. Figure 1.1 presents a block diagram of the experimental setup. The dome shaped flight simulator [26] has been used to perform open-

and closed-loop experiments. In open-loop experiments the insect would not have control over the visual stimulus. In the closed-loop scenario the analog voltage values generated from conversion of depressor asymmetry time difference and wing beat frequency would control the visual stimulus, thus giving the insect control of the visual stimulus. The visual stimulus used for closed-loop experiments was a 'Cube', a detailed description of which has been provided by Arkles in [29].

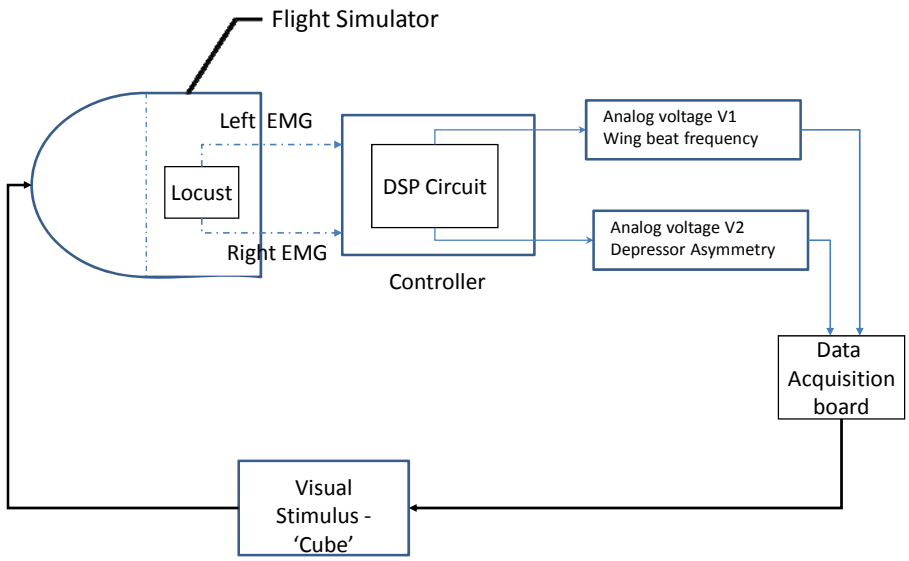

Figure 1.1 Experimental setup. The insect is placed inside the dome shaped flight simulator. In open-loop scenario the insect has no control of the visual stimulus ('Cube'). In closed-loop scenario analog voltage values V1 and V2 obtained from conversion of wing beat frequency and depressor asymmetry time difference control the visual stimulus, thus giving the insect the ability to control the visual stimulus.

Objectives:

The objectives of the experiments described here were:

a) To design a circuit to process EMGs obtained from depressor flight muscles of an insect and determine the depressor asymmetry time difference and wing beat frequency. Use the

depressor asymmetry time difference and wing beat frequency as parameters for feedback control.

b) To test the circuit in open-loop and closed-loop experiments.

A brief introduction of the methods adopted to study insect flight is provided in Chapter 2, and a detailed explanation is given for selecting the locust as the model system to perform this work. Therefore, information about locust physiology and the requirements to perform open-loop and closed-loop experiments using locusts are discussed.

Chapter 3 in this work provides detailed description about the design procedure for the feedback control circuit to process EMG signals. The results obtained by testing the feedback control circuit using both open and closed-loop protocols are presented in Chapter 4. Discussion of the results obtained and the performance of the feedback control circuit, its limitations, and the potential applications of the work are described in Chapter 5.

CHAPTER 2

BACKGROUND

Flight control in insects has been studied extensively; however the underlying neural mechanisms are not fully understood. An insect's behavior can be understood as dynamic in its natural environment. This dynamic behavior corresponds to the ever changing patterns of environmental stimuli. Various insect model systems have been used to understand neural mechanisms that try to elucidate this adaptive behavior. The goal of this ongoing research focusing on the neural control of insect flight is to understand the manner in which sensory information is being integrated within the central circuitry that modifies and coordinates motor output. Inspired by the structure and function of the visual system and insect brain, various flight control, navigation systems and collision avoidance systems have been proposed and are in the process of development. This set of insect flight control includes various model insect species, including the Hawkmoth *(Manduca sexta)* [8,26], Dragonfly *(Odonata)*, Fruitfly *(Drosophila melanogaster)* [1,20,21,22,23,24,25] and Locusts *(Locusta migratoria L.*) [2,5,6,9,10,11,12, 13,14,15,16,17,18,19].

2.1 Open-loop and closed-loop concept

Insect flight research has focused on stimulus detection and perception, sensory motor integration and motor outputs that contribute to describe flight behaviors well [1-3,5-28,33]. Studies involving the locust as a model system have been carried out to understand the flight motor pattern and the prevailing sensory input that could alter the flight pattern [2-3,5-7,9-20,27-28]. Most of these studies investigating locust flight kinematics using tethered locusts have focused on the open and closed-loop experimental approach [2,3,5-7,11].

In control theory an open-loop system is a system lacking feedback control. Such a system is governed or controlled directly and the changes in the system parameters are not accounted for. On the contrary, the closed-loop system contains a feedback loop. This feedback can be understood as a process whereby some proportion of the output signal of the system is fed back to the input. A change of some of the environmental conditions during locust flight may also produce a change in functioning of its motor control system. The sensory inputs of the feedback loop of a locust could be considered as formed by a combination of its compound eyes, the ocelli, the antennae, wind sensitive head hairs and the flight motor neurons [30]. Various parameters that may be required to be maintained during the flight of a locust may be recorded by its nervous system and conveyed to a regulation module in terms of motor output.

2.2 Flight Simulators

Flight simulators have been used to a greater extent to investigate behavioral responses of neurons to visual stimuli for various insects [1-3,5-7,9-19,22-27]. The objective of these flight simulators has been to provide the experimenter with an ability to simultaneously present a computer-generated visual environment and record neuronal activity and/or behavioral data. These flight simulators combine a realistic and interactive visual environment with mechanosensory and olfactory stimuli and have been effective in addressing questions of insect flight, providing the ability to perform experiments in open-loop and closed-loop conditions [26]. Using flight simulators, both open and closed-loop experiments have been performed for insects like flies, moths and locusts [1-28].

2.2.1 Locust as an insect model:

The brain of flying insects includes principles of visual flight control that are highly effective and efficient in terms of their implementation [4,31]. A smaller number of neurons in the invertebrate nervous system exhibits lesser levels of complexity compared to a vertebrate nervous system. In spite of being fewer in quantity but being larger in size than the neurons in mammals, the neurons in an insect's nervous system permit researchers to easily insert electrodes and obtain physiological recordings [32]. The locust's nervous system shares the advantages of invertebrate's nervous system and has been used to address questions of insect flight and sensorimotor integration. Locust flight can be characterized as being repetitive and exhibiting a rhythmic wing movement. The locust flight system has proven to be an excellent model for the investigation of mechanisms underlying the control of locomotion, and has inspired development of prototype Unmanned Aerial vehicles (UAV), which also incorporate the features of a collision avoidance neuron Lobula Giant Movement Detector (LGMD) neuron [4,33,34].

2.2.2 Locust physiology

Locust flight is produced by the flapping of its forewings and hindwings. A group of 10 muscles that are innervated by a specific set of motor neurons controls each wing [32]. The wing movement is controlled by an alternating pattern of contraction of the elevator and the depressor muscles. These muscles either attach directly to the base of the wing or indirectly cause wing movements by deforming the thoracic exoskeleton. The muscles can be divided into 3 different categories: 1) Direct flight muscles that are inserted directly onto the wing, 2) Indirect flight muscles responsible for wing movement produced by distortion of thorax shape and 3)

Accessory muscles that are responsible for twisting movements of the wing and also for altering the effects of other muscles [32]. The set of elevator muscles that are vertically arranged are responsible for the upward movement of the wing, whereas the depressor muscles that are arranged horizontally and vertically are responsible for the downward stroke of the wing. The vertical depressor muscles, the basalar and the subalar power the downstroke of the wing and are responsible for controlling the wing twisting [32]. The locust muscles are activated neurogenically and hence a single action potential in a motor neuron evokes a single twitch contraction and wing movement. The muscles m97 and m98 are the forewing first and second basalars, respectively. Muscles ml27 and m128 are the hindwing first and second basalars, respectively. Muscle m99 is the forewing subalar, and ml29 is the hindwing subalar muscle [32]. Muscles m81 and m112 are the indirect depressors located in the forewings and hindwings respectively. Muscles m83, m84, m89, m90, m91 and m103c are the elevator muscles located in the front wing whereas m113, m118, m119 m 120 and m133c are elevator muscles located in the hindwing [32]. Accessory muscle m85 is located in the forewing and m114 is located in the hindwing [32]. Figure 2.1 provides details about the location of the locust flight muscles.

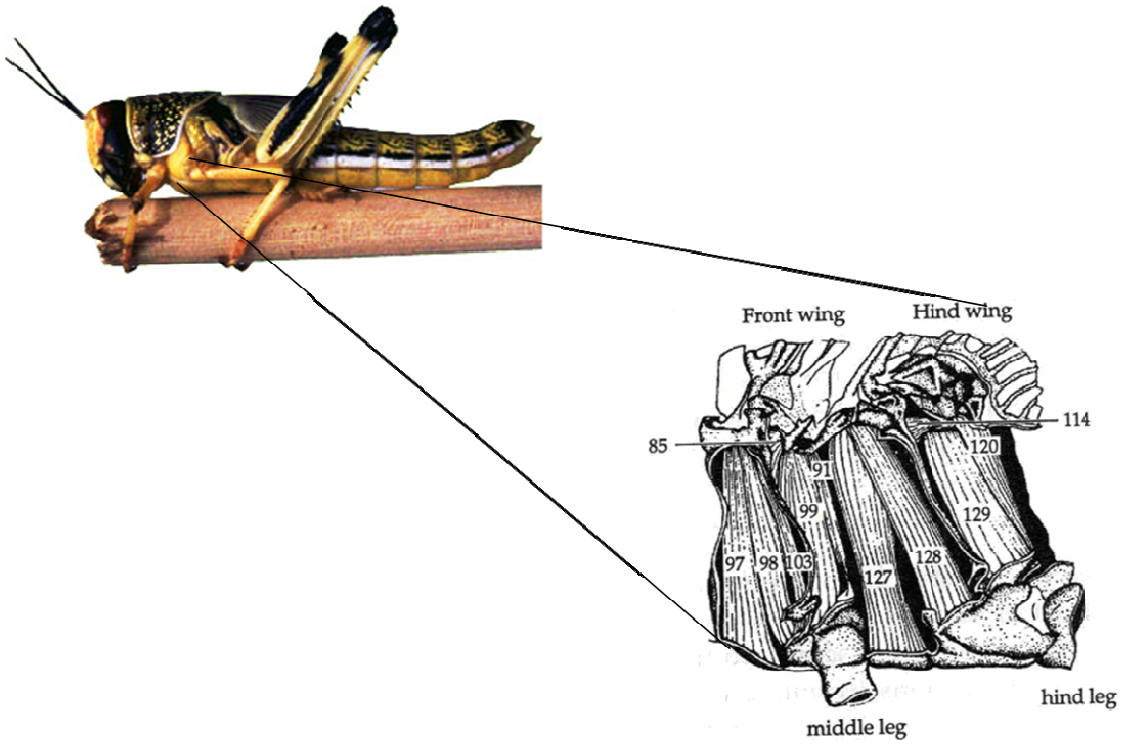

Figure 2.1 Arrangement of Locust flight muscles. The image shows the arrangement of forewing and hindwing first and second basalar muscles (m97 and m98 - both forewing, ml27 and m128 both hindwing). Fore and hindwing subalar muscles (m99 and m129 respectively) are also visible. m91 and m103c are the elevator muscles located in the front wing. Locust image modified from [35]. Image showing flight muscles modified from ([32], page 482, Chapter 11, Figure 11.3).

2.2.3 Locust flight pattern:

Basic aspects of locust flight motor pattern have been investigated by recording electrical activity of flight muscles [17]. Physiological recordings like electromyogram signals reflect motorneuronal output and hence have been used extensively for studying locust flight. For neurogenic flyers like locusts, EMGs obtained from their muscles suggests that locusts exhibit a stereotype muscle contraction during flight. Figure 2.2 displays EMG signals acquired from first basalar (m97) depressor muscles. This flight motor pattern comprises the alternating activity of elevator and depressor muscles. Locusts possess frequency coupled wings (identical wing beats

in fore and hind wings). Synchronous wing movement is achieved by simultaneous firing of elevators followed by depressors of the left and right wings of a pair [32]. There is a small time difference between the movement of the hind and the fore wings [19]. The hind wings lead the forewings by a time of 5~10 ms and hence the wings of locust are not phase coupled [19]. Alternating bursts with a frequency of 20 Hz have been observed in the spiking of the elevator and depressor muscles from one wing [32]. The forewing direct depressor muscle m97 fires earlier than any other forewing depressor muscle. The firing pattern observed for m97 indicates that during straight flight double spikes (doublets) or single spikes are visible [17]. The m97, m98 and m127 muscles are responsible for pronation and depressing the wing. During downstroke the muscle m85 functions to counteract the pronation [17]. Also during downward stroke in a straight flight, the m127, m128 (basalars from the hind wing and the subalar m29 fire earlier than forewing direct depressor muscles [17].

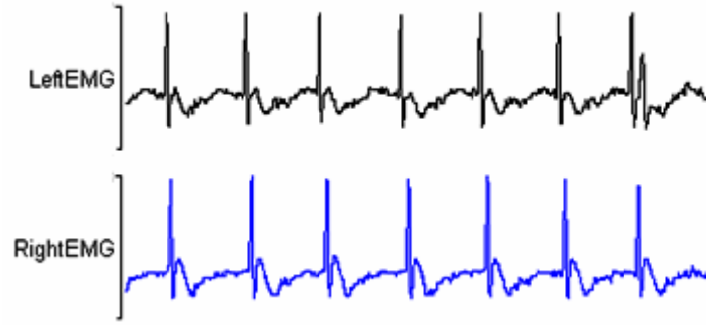

Figure 2.2 EMG signals. The figure shows EMG signals (muscle action potentials) acquired from first basalar (m97) depressor muscles located in the left and right wings.

2.3 Open-loop and closed-loop experiments using flight simulators

Knowledge about the basic principles of locust flight has been gained by performing tethered flight experiments in open and closed-loop conditions. It has been reported by Robert [10] that a free flying locust may react in different ways on sensing a change in its visual world. Robert [10] has suggested that the locust may deviate from its pre-planned path or use its

feedback loop to perform compensatory maneuvers. Here the closed-loop paradigm was based on steering torques being used to control visual stimuli. Rowell [11] has presented a review of neural circuits that regulate steering movements in the locust. Rowell [11] has suggested that the central nervous system of the locust can be thought of as an 'autopilot'. The information gathered by the locust's sense organs has been known to evoke offsetting motor responses to restore the deviation from the straight course. Rowell [11] has also suggested that this 'autopilot' may be disabled in cases of spontaneous changes in the natural world and may result in intentional steering.

Cruse et al. [30] have suggested that the term open-loop can be understood as any steering effort a locust might produce during tethered flight that has no effect on its position whether in a wind tunnel or wind stream. Since under natural conditions sensorimotor integration is closely linked, a closed-loop experiment may try to address questions about steering actions (intentional and correctional) during free flight of the insect. Berger and Kutsch [12] and Kutsch et al. [36] have advocated that closed-loop experiments with visual stimulus may tend to elucidate the free flight of locust. Robert [10] has performed closed-loop experiments using tethered locusts that were presented with simulated *'reafferent'* steering information based on the concept that was used by Reichardt and Wenking [20] and has been modified further. Baker [2] has presented a flight simulator concept, which simulated closed-loop condition around the yaw axis in tethered flying locusts. Results from the work by Baker [2] indicate that under closed-loop conditions the subjects (locusts) reacted to visual stimulus and interacted with it similar to that observed during free flight conditions. Robert and Rowell [5,6] have shown that under closed-loop conditions locusts, flown in a flight simulator, converted the steering force into motion and using steering maneuvers controlled the visual environment similar to open-loop

conditions. Under the closed-loop situation the *'yaw torque meter'* signals were used to control the speed and direction of rotation of the servomotor [5,6]. Möhl [7] has suggested that an asymmetrical flight pattern of a locust was a function of short-term flight experience. The results obtained by Möhl [7] were based on an experimental paradigm that used the closed-loop concept, where the timing of two contralateral depressor muscles was used as an input (feedback) to the yaw angle with which the locust would fly in a wind tunnel. Under this closed-loop paradigm the flight muscle activity was used to control the visual stimulus. The results indicated that under closed-loop conditions the locusts were able to align themselves straight ahead against the air in a wind tunnel.

The work presented here deals with the flight simulator that has been described by Gray et al. [26]. The closed-loop experiment performed by Gray et al. [26] can be described as one, where the movement of the computer generated environment is controlled by using a photodiode sensor that would optically sense movements of the insect's abdomen. Gray et al. [26] have highlighted the limitations of other flight simulators, based on the concept of interactive visual stimulation governed either directly by neurological activity or by insect movement and not permitting the insect to maneuver in a simulated environment. They have argued that closed-loop experiments (based on integrated sensory motor feedback) where the sensory feedback loop is accounted for can be very useful to present multi-sensory stimuli and also record neurophysiological activity. Robert [10], Berger and Kutsch [12] have suggested that restriction, in the form of tethering of the insect's free movement may reduce or alter the integration of sensory information under natural conditions.

2.4 Steering action in locust flight

For a locust to steer during flight it needs to adjust its wing movement and coordinate movements of other body parts. The various mechanisms that help the locust to steer are required to address the variable parameters like nonlinearities in neural and muscular mechanism, the unpredictable environment, the voluntary turns that may be required, and also correct the deviation of flight path arising due to above reasons [32]. This steering mechanism of the locust has been studied extensively and has been categorized into a) “Correctional steering” and b) “Intentional steering” [11].

The “correctional steering” mechanism can be understood as one resulting from unintentional or involuntary deviations from course; required to have stable movements against turbulent changes of air and for corrections of motor errors [32]. The “correctional steering” mechanism also stabilizes the movement of the visual world over the eyes, thus reflexes act to compensate for unintentional course deviations. The “intentional steering” movements are those that are exhibited to avoid an obstacle in the flight path and hence can be understood as a locust’s response to external stimuli. The steering movements are defined about three main axes of the locust’s body a) pitch - vertical body movement with head pointing either in upward or downward direction b) roll - locust body movement either clockwise or counterclockwise about its dorsolongitudinal axis of the body c) yaw - movement of body in horizontal plane about the dorso-ventral axis (an axis perpendicular to the wings), in which the head movement is towards the left or right of the abdomen. These terms are well defined for an aircraft and therefore can be understood by relating the locust to an aircraft.

There are considerable differences between the “correctional” and “intentional” steering maneuvers exhibited by the locust. Rowell [11] reported that during “intentional steering”

locusts move the head in the opposite direction of the turn, and vice - versa during “correctional steering”. Also, Robertson and Reye [3] have reported that the “correctional steering” is not characterized by profound Forewing Asymmetries (FWA) that are observed during “intentional steering”. These FWA have also been observed during “intentional steering” actions in response to heat stimuli [14], and auditory stimuli in the form of bat echo or vision [13]. The FWA can be described as difference in angle of elevation on either side of the locust body, i.e., the angular difference created by the right and left forewings with respect to the dorsal - ventral axis of the body [13].

Shoemaker and Robertson [28] have reported that large asymmetries observed in the angle of elevation of the forewings during downwards stroke result from the *“bulk shifts”* in the activation times of forewing depressor muscles. These *“bulk shifts”* can be referred to the advancement of timing of all depressor muscles located in the forewing on one side of the body with respect to the corresponding contralateral muscles. During turning maneuvers, asymmetries are observed in the timing of firing of the right and left forewing first basalar (m97) depressor muscles [28].

2.5 New approach to perform closed-loop experiments

Often locusts perform gliding behavior during free and tethered flight. It has been observed that locusts exhibit gliding behavior when challenged with a looming stimulus during tethered flight [37]. This behavior is marked by a drop in mean wing beat frequency and indicates a descent in the flight altitude during free flight [37]. The gliding and turning maneuvers may not entirely rely upon the abdomen movement. Hence, a better method to understand the kinematics of locust flight and flight control during a closed-loop experiment is required. As mentioned earlier, during turning maneuvers, asymmetries are observed in the

timing of firing of the right and left forewing first basalar (m97) depressor muscles. We present a novel method that utilizes asymmetrical timing of bilateral depressor muscles, the forewing first basalars (m97), of the locust to close a visual feedback loop in a computer-generated flight simulator. The method converts the time difference between left and right m97s to analog voltage values.

The flight simulator and the experimental approach described by Gray et al. [26] permitted them to investigate neuronal activity during realistic flight steering, which had not been addressed by other methods probably due to technical limitations. They performed experiments in closed-loop conditions using moths as test subjects, by detecting the insect's abdomen, which in turn controlled the movement of the visual environment. The research work presented in this thesis uses the same closed and open-loop experimental protocol with tethered locusts but does not use the photodiode sensor used by Gray et al. [26].

CHAPTER 3

MATERIALS AND RESEARCH METHODS

3.1 Experimental animals

Subjects for these experiments were adult male *Locusta migratoria L.* The Locusts were obtained from a colony maintained in the Department of Biology at the University of Saskatchewan. The experiments were performed at room temperature, approximately 25 ~ 28 °C.

3.2 Animal preparation

The legs of the animal were removed to prevent interference with the EMG electrodes. After removal of the legs, a rigid tether was attached to the ventral surface of the thorax using low melting point beeswax. EMG electrodes were used to record right and left m97 activity. The EMG electrodes consisted of fine copper wire (100 μm in diameter) and were insulated except at the tip. Each electrode was held in place using a small drop of wax. A silver wire electrode, inserted into the sternum served as a reference electrode. The tethered animal was then placed in the flight simulator facing the apex of the dome, giving it enough room to move its wings and avoid contact with the inserted electrodes. Figure 3.1 provides details about insertion of electrodes and m97 Depressor asymmetry.

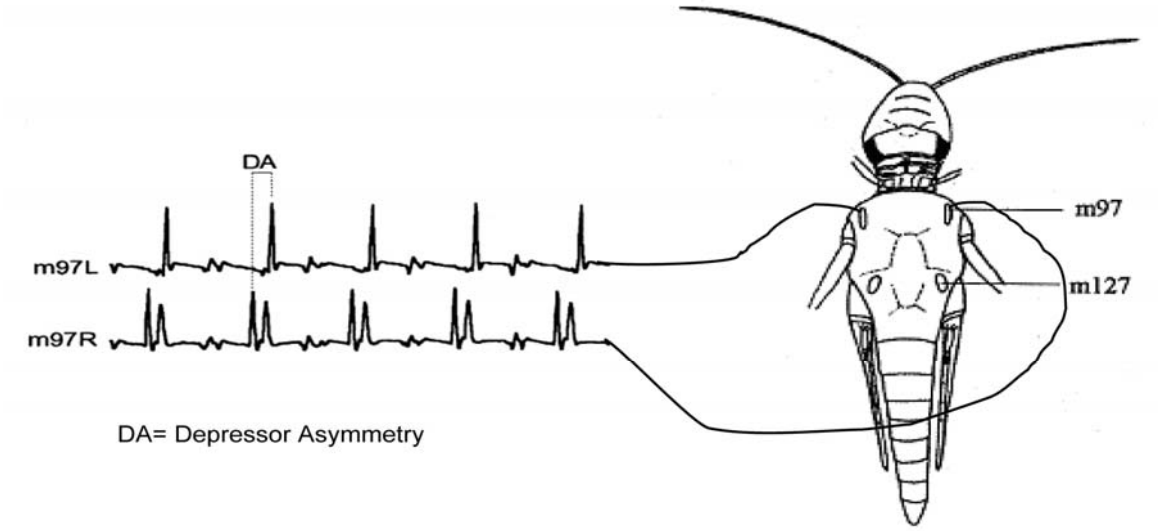

Figure 3.1 Schematic diagram showing insertion of electrodes into m97 depressor muscles and the DA time difference. The top trace denotes EMG signals acquired from the left wing. The bottom trace denotes EMG signals acquired from the right wing. DA is the depressor asymmetry. (Modified from Shoemaker and Robertson [28], page 479, Figure 1B)

3.3 Data acquisition system

A differential amplifier (A-M systems, Differential AC Amplifier Model 1700) was used to acquire 2 channels of EMG signals. The analog signals were channeled to the main data acquisition and signal processing system provided by Tucker Davis Technologies Ltd. (TDT, Alachua, FL, USA). This data acquisition and signal processing system is termed as 'System 3' TDT [38]. We used a 'RX5 Pentusa base station' and 'RP2.1 Real-Time Processors' to record and process, on line, m97 activity.

3.3.1 'RP2.1 Real-Time Processors' and 'RX5 Pentusa Base station'[38]

TDT's System 3 utilizes signal processing modules, 'RP2.1' real-time processors and 'RX5' [38]. The 'RP2.1' and 'RX5' processors consist of 'SHARC'® category floating point digital signal processors (DSPs). The 'RP2.1' belongs to the 'RP' [38] family, which are based

on the single DSP architecture whereas the 'RX5' belongs to the multi-DSP architecture. The processors belonging to either family can be configured and controlled using 'circuits' that are designed with the 'RP Visual Design Studio (RPvdsEx)' [38]. 'RX5' 'Pentusa' base station consists of either two or five digital signal processors (DSPs). The advantage of using a multi-DSP system is obtained in terms of equal distribution of processor tasks and efficient data transfer to the PC. In the multi-DSP feature, one DSP acts as a master (main) DSP while the others act as auxiliary DSPs. The data acquisition and signal processing system used by us allows the user to acquire up to 64 channels of broadband data [38]. Figure 3.2 presents a block diagram of the data acquisition system and the general layout.

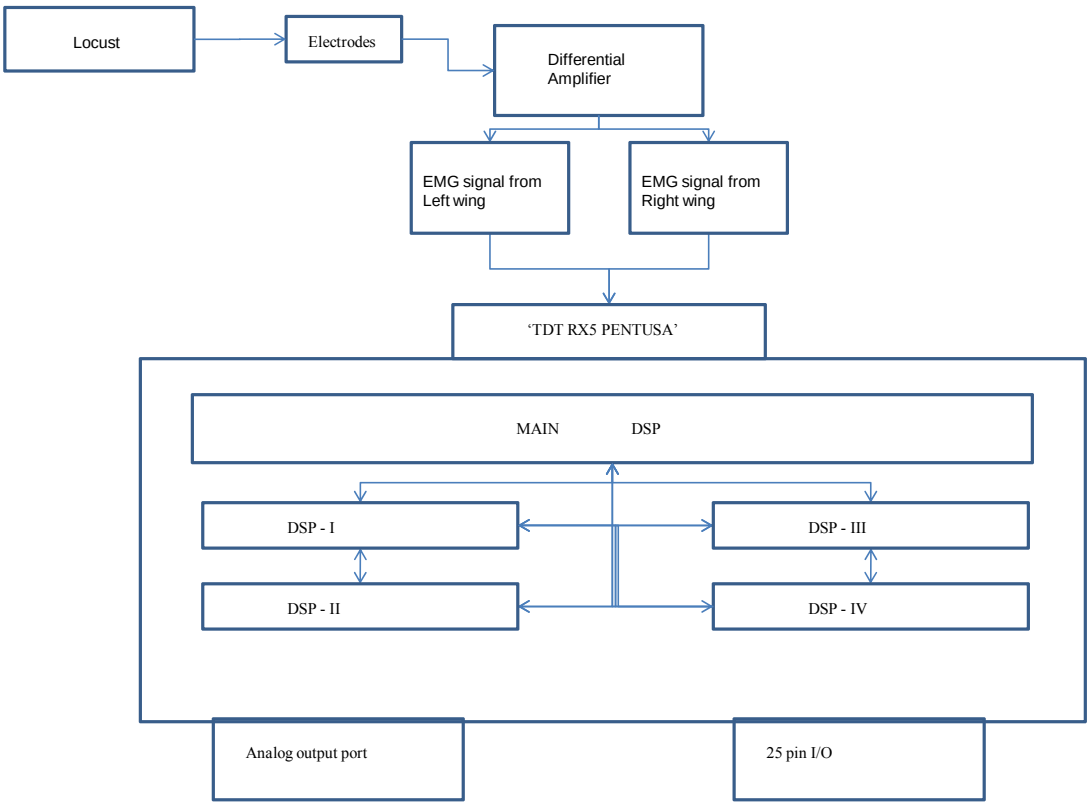

Figure 3.2 Block diagram of data acquisition system. The EMG signals acquired from the depressor muscles were acquired by the differential amplifier. These signals were channeled to TDTs 'RX5' 'Pentusa' system.

The feedback 'circuit' was designed in Real-Time Processor Visual Design Studio ('RPvdsEx') provided by TDT. This is a graphical design interface which includes various components that can be programmed to perform various signal processing tasks. It allows the user to create desirable processing functions in the form of 'circuit' diagrams. The 'RPvdsEx' software stores the 'circuit' diagrams in the form of pages. This 'circuit' diagram when compiled in the software generates a DSP code that can be executed from within the same environment or from other TDT software [38].

‘OpenEx’, a software suite, was used for multi-channel data acquisition and controlling the experiment in real-time. This software allows the user to control various experimental parameters with the help of ‘parameter tags’. It comprises ‘OpenWorkbench’, ‘OpenBrowser’, ‘OpenScope’ and ‘OpenController’[38]. The interface between ‘OpenEx’ and the hardware is provided by ‘OpenWorkbench’. ‘OpenWorkbench’ provides the user with a graphical user interface and options to select the devices and processors for the experiment and type of data to be stored. ‘OpenController’, which is a visual interface for designing and implementation of custom control sets, was used for these experiments because it allowed the user (experimenter) to set and control the parameter variables and acquire data sets in real-time [38]. Control of experimental parameters such as cut-off frequencies for filters, threshold settings for spike sorting, and signal selection from multiple channels was made possible by using ‘OpenController’. It also permits the user to read and display precise parameter values. Figure 3.3 presents a screen capture of ‘OpenController’.

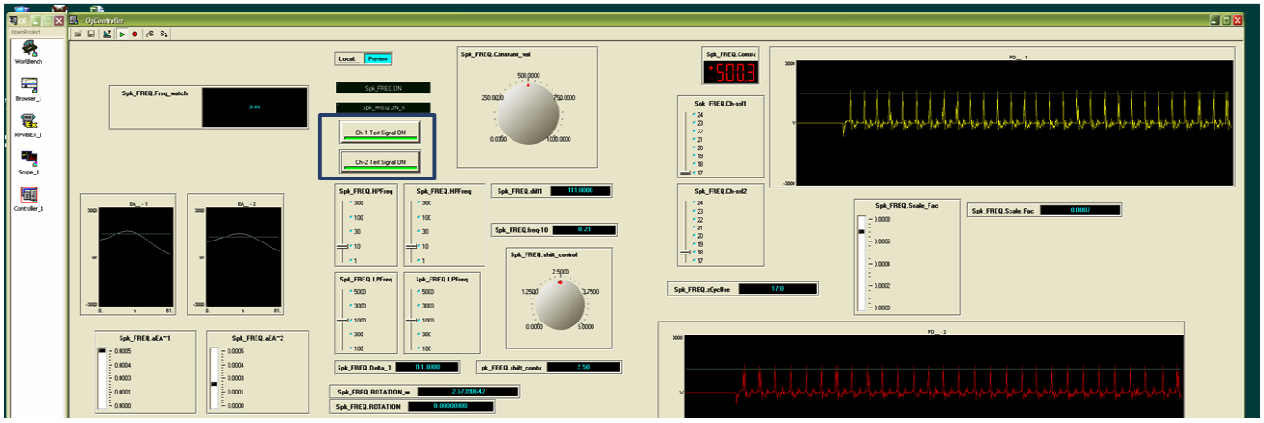

Figure 3.3 Screen capture of 'OpenController'.

3.4 Basic Trigger and Timing Control 'circuit'

Continuous EMG signals and sorted spikes needed to be acquired. Hence, it was imperative that we had main trigger and clock generator constructs that would provide sufficient triggering and timing control to acquire data continuously. As per the conventions used in the 'RPvdsEx' and 'OpenEx' software, a global trigger was required that would ensure the simultaneous activation of all the devices for the TDT system [38]. This task of global trigger and timing control 'circuit' was assigned to the main DSP. A clock generator was designed using the 'SimpCount' (simple counter) component. The output of the 'SimpCount' - 'iTime' was made accessible to all the DSPs. Detected spikes were assigned time stamps via the 'iTime' line. Here the time value is measured in the number of samples from the instant the 'Reset' line went high and is automatically converted to seconds by 'OpenWorkbench' when time stamping data [38]. Figure 3.4 presents a block diagram of the trigger and timing control 'circuit' that was created and allocated to the main DSP. It has been mentioned earlier, that the 'RPvdsEx'

software stores the 'circuit' diagrams in the form of pages. Appendix A (Figure A.1) provides detailed 'circuit' diagram for the basic trigger and timing control 'circuit'.

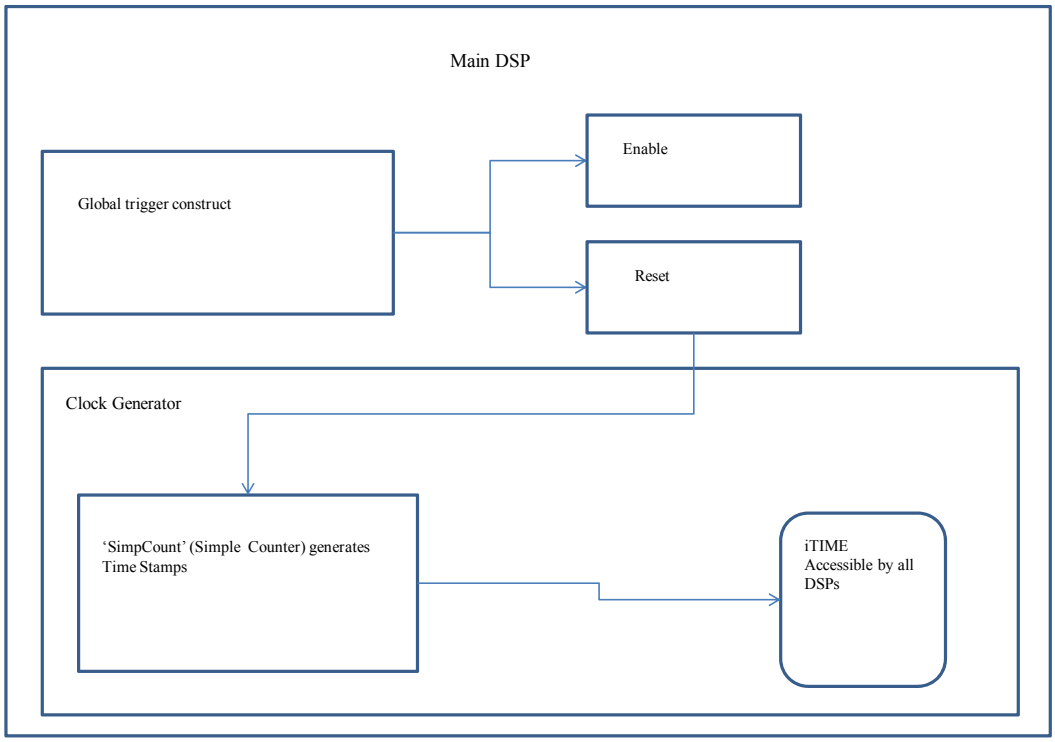

Figure 3.4 Block diagram for the basic trigger and timing control construct. Clock generator was created using 'SimpCounter' (Simple counter). To ensure that the clock started at zero the 'SimpCount' received input from 'Reset' line of global trigger construct. Output of 'SimpCount' referred as 'iTime' was made accessible to all the DSPs to assign timestamps.

3.5 EMG signal filtering

The ‘circuit’ after being designed was intended to work for a variety of physiological signals. It was decided to test the ‘circuit’ with pre-recorded EMG signals, which were stored in wave file formats. This required modification in the original ‘circuit’ and hence a multiplexer was used. The TDT software provides the user with two multiplexer components a) ‘MuxIn’ [38] and b) ‘MuxOut’ [38]. The ‘MuxIn’ permits the user to have 4 signals as inputs and has a channel selector, controlled by the user via ‘OpenController’ in real-time. Switches ‘Ch-1 Test Signal ON!’ and ‘Ch-2 Test Signal ON!’ were created in the ‘OpenController’ that allowed us to swap between pre-recorded EMGs and EMGs that are acquired in real-time (refer Figure 3.3 highlighted rectangle). These switches controlled the channel selector for the ‘MuxIn’ component using ‘FakeSel~1’ and ‘FakeSel~2’ parameter tags. This output from the ‘MuxIn’ which can be an EMG signal (either a pre-recorded or obtained in real-time) was labeled as ‘RawSig1’ for Channel 1 and ‘RawSig2’ for Channel 2. Channel 1 represented EMG signals acquired from left wing and Channel 2 from right wing. A block diagram of the above process has been presented in Figure 3.5.1. Appendix B (Figure B.1) represents page-2 of the software containing detailed ‘circuit’ of the process described above.

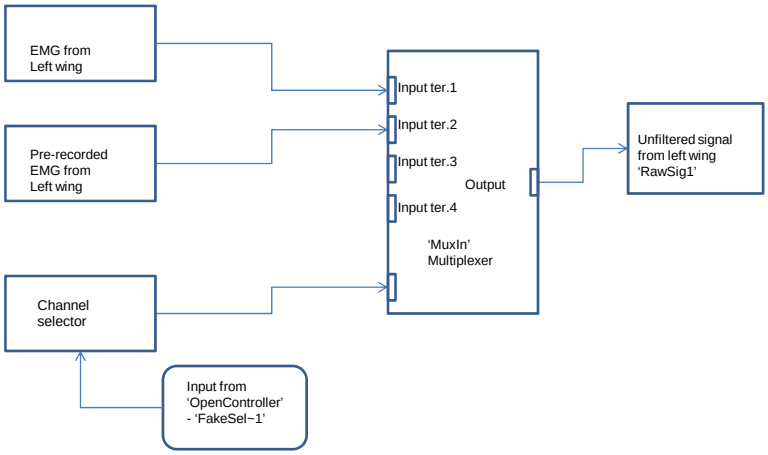

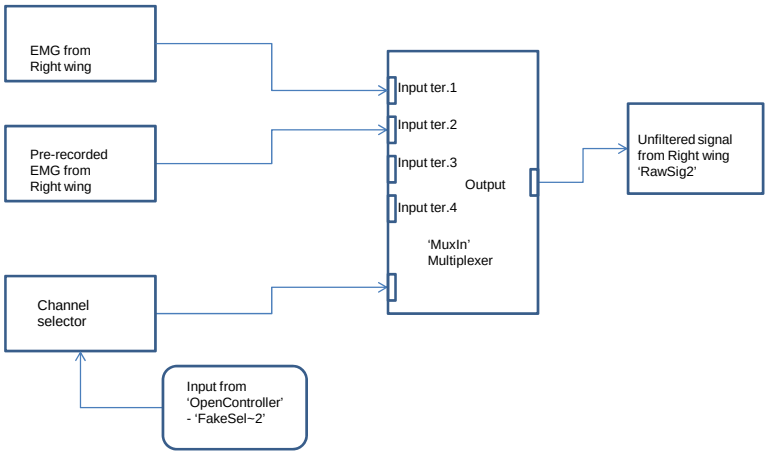

Figure 3.5.1 Block diagram for signal acquisition process and use of multiplexer components. It is a representation of circuit diagram provided in appendix B (Figure B.1). The multiplexer components provided the flexibility to select a signal from wave file or a live animal.

These physiological signals were sampled at 25 KHz/channel. The sampled signals were then filtered using low-pass and high-pass filters. The 'ButCoef1' available in the software permits the user to build second-order Butterworth filters. The 'Biquad' component available in the software was used in conjunction with 'Butcoef1' component to create high-pass and low-pass filters. The filter coefficients for these high pass and low pass filters were generated using the 'ButCoef1' component.

In the 'OpenController' 'sliders' were created to control and set cut-off frequencies for these filters in real-time. The cut-off frequencies for these filters adjustable in real-time were set to 10 and 1000 Hz for high-pass and low-pass respectively. The 'sliders' would send the value of the cut-off frequency (set by the user) to the 'ButCoef1' component's 'Fc'- cut off frequency input terminal using parameter tags while the chain is running (i.e. the 'circuit' being compiled and the processor is in the 'run' mode). Once the cut-off frequencies were set using the 'sliders' in 'OpenController' they were not altered.

A block diagram representation of the above process has been presented in Figure 3.5.2. Appendix C (Figure C.1) represents page-3 of the software containing detailed 'circuit' of the above process.

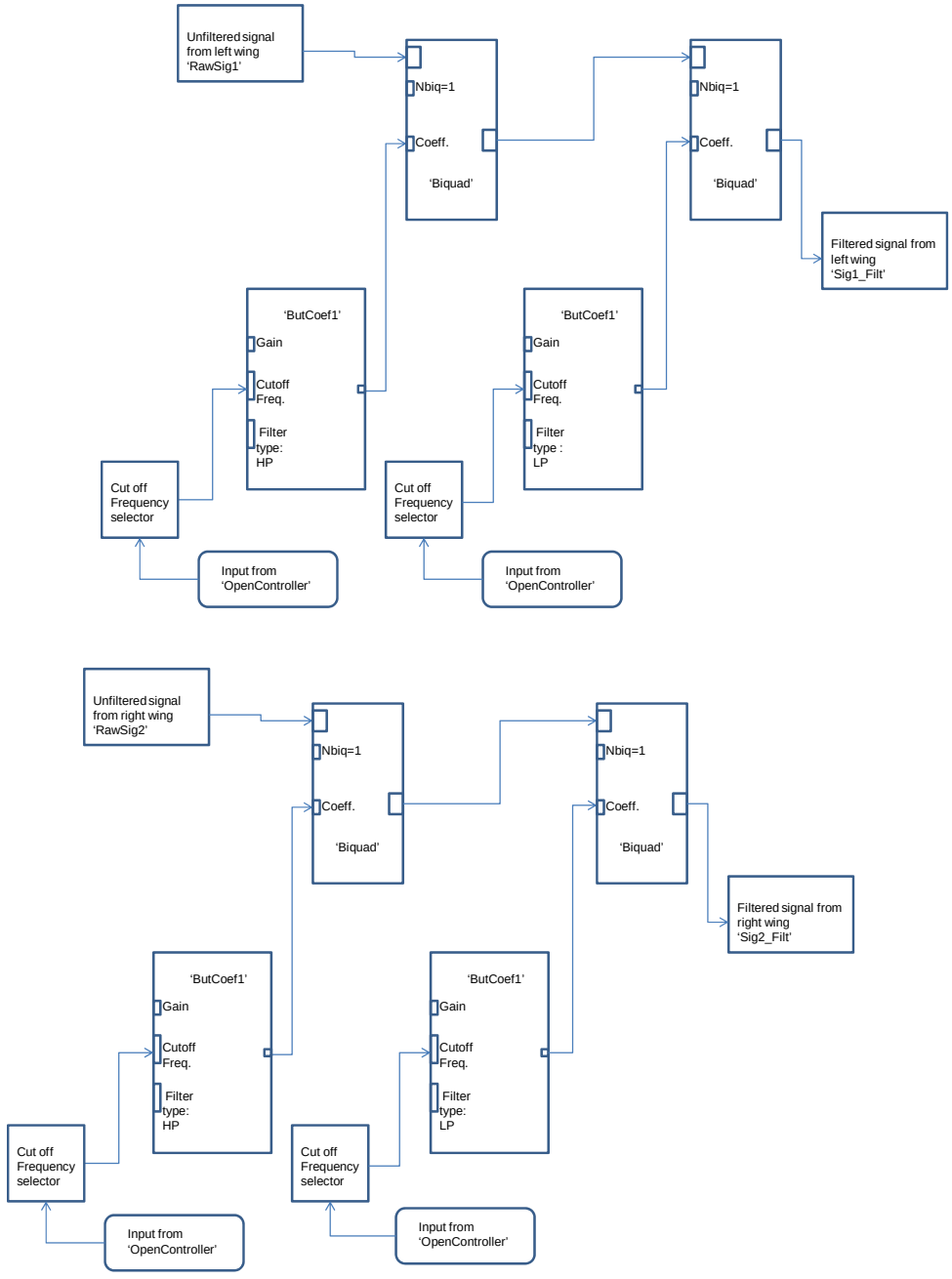

Figure 3.5.2 Block diagram depicting the filtering process for the EMGs acquired from left and right wing. The unfiltered signals referred as 'RawSig1' & 'RawSig2' from left and right wings respectively were filtered using high-pass and low-pass filters. These Butterworth filters were created using the 'ButCoef1' and 'Biquad' components available in the software. The cut-off frequencies for high-pass and low-pass filters were set to 10 Hz and 1000 Hz using sliders in 'OpenController' and were unaltered. The filtered signals from the left and right wings were referred as 'Sig1_Filt' and 'Sig2_Filt' respectively.

'Sliders' in the 'OpenController' were named as 'Spk_FREQ.HPFreq' and 'Spk_FREQ.LPFreq' for high-pass filters and low-pass filters respectively. Four sliders were used, i.e. a pair of high-pass and low-pass filters for each channel. Figure 3.5.3 which is a modification of Figure 3.3 highlights the 'sliders' (see rounded rectangle) created in 'OpenController'. Thus we obtained filtered EMG signals from the left and right wing of the locust. The filtered signal from the left wing was labeled as 'SIG1_FILT' and that from the right wing was labeled as 'SIG2_FILT'.

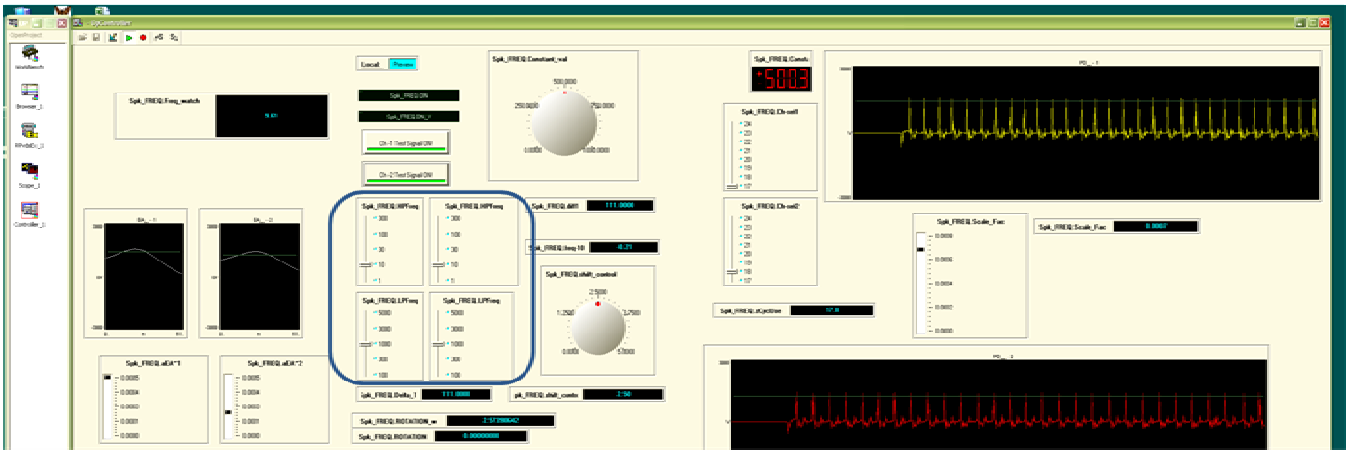

Figure 3.5.3 Sliders in 'OpenController'. The rounded rectangle highlights the sliders designed to set the cut-off frequency for the high-pass and the low-pass filters.

3.6 Spike detection on both channels

3.6.1 Spike detection for Left and Right wing EMG signals

Having obtained the depressor EMG signals, the next step was to perform spike detection. For neurogenic insects like locusts, a spike is the consequence of a motor neuron firing. We were interested in identifying the event, when a spike was generated from the left and right wings and assigning a time stamp to it. Since depressor EMGs obtained from locusts are of sufficiently distinct amplitude, an application of a simple linear threshold is sufficient to identify spikes rather than analyzing neural spike train data. This spike detection was to be performed in real-time using TDT hardware and software, and hence it was necessary that the user had complete control over the spike detection process. It was necessary to create controllers in 'OpenController' that would enable the user to achieve that goal.

The TDT software provides the user with options of selecting various neuroanaylsis components. 'SortSpike2', 'Sortspike3', and 'FindSpike' were available for our use [38]. For our experiments the 'SortSpike2' component was chosen. The objective of spike discrimination and detection was achieved from 'OpenController' using the 'Scrolling Threshold control'. Figure 3.3 with modifications has been reproduced as Figure 3.6.1 wherein the highlighted rounded rectangles display the 'Scrolling Threshold control' [38].

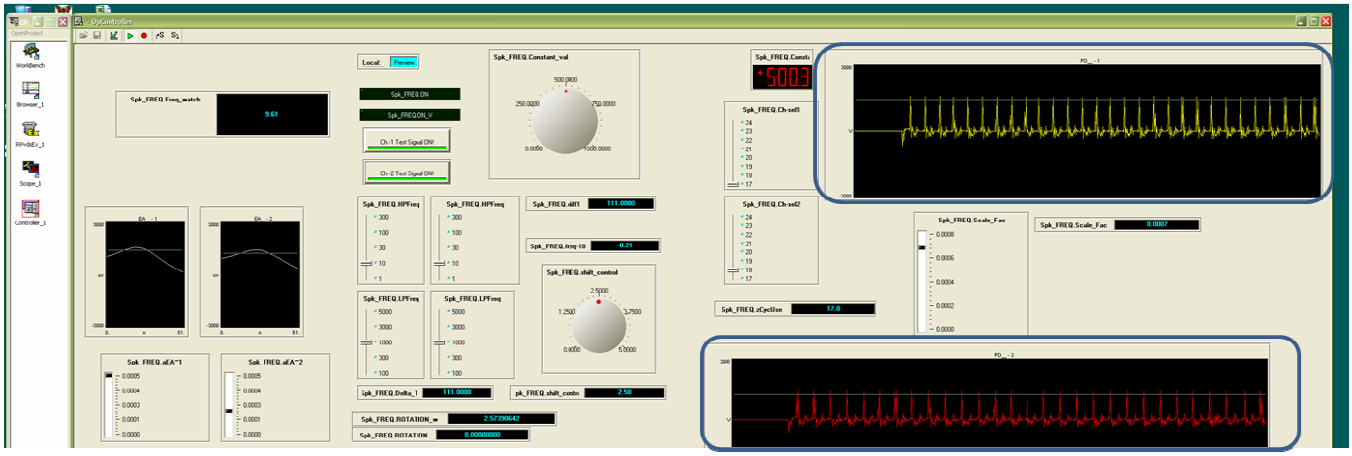

Figure 3.6.1 Screen capture of ‘OpenController’, the rounded rectangles refer to the ‘scrolling threshold controls’.

The ‘SortSpike2’ component received the filtered EMG waveform as an input and had detected spikes as its output. For this ‘circuit’ design, two ‘SortSpike2’ components were used, one for each channel (i.e., one each for channel carrying EMG from left and right wing). The ‘SortSpike2’ component for channel 1 received input from ‘SIG1_FILT’ that carried the EMG from the left wing. ‘SortSpike2’ for channel 2 received input from ‘SIG2_FILT’ that carried the EMG from the right wing.

The ‘SortSpike2’ is provided with a parameter; ‘Thresh’. The user can set and control the ‘Thresh’ parameter by setting the threshold voltage (window) in real-time using ‘sliders’ in ‘OpenController’. Figure 3.6.2 is a reproduction of Figure 3.3 with modifications and shows the ‘Scrolling Threshold control’ (highlighted rounded rectangles) [38]. The horizontal bar (highlighted with ellipses), visible in the figure would set the threshold value. The ‘sliders’ (highlighted with a rectangle) would control (set) the horizontal bar (highlighted with ellipses), and in turn communicate the value to the ‘Thresh’ parameter of ‘SortSpike2’ in real-time using

parameter tags. Potential spikes were defined as those, which would cross the fixed voltage threshold inside 'SortSpike2' [38].

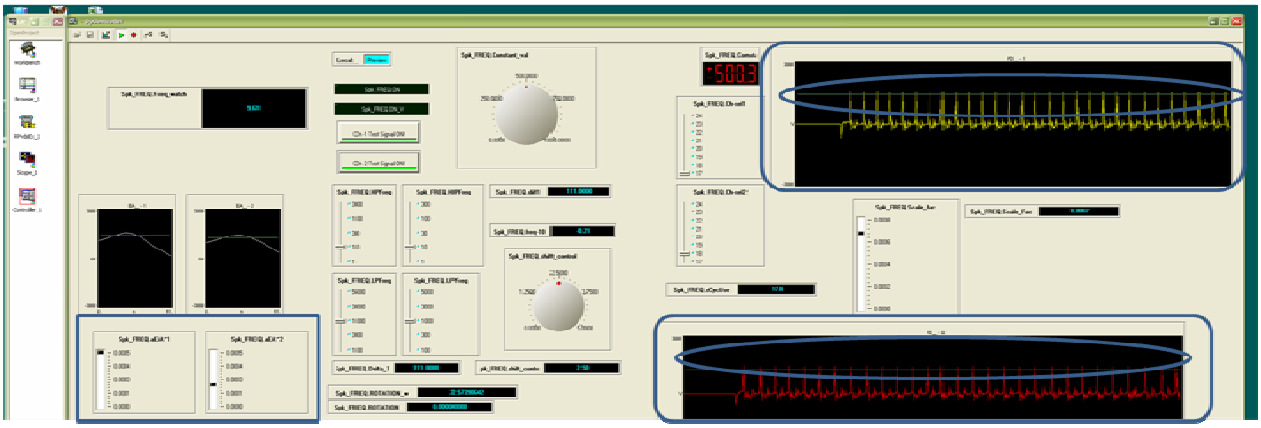

Figure 3.6.2 Screen capture of 'OpenController'. The sliders (highlighted with a rectangle) would control the horizontal bar (ellipses highlighted) setting the threshold voltage for detecting spikes.

The 'SortSpike2' component has an input parameter; 'Tag'. The 'Tag' parameter received input from the 'iTime' (the time stamp). When a potential spike was detected it was tagged with the value received by 'Tag' (the time stamp in this case). 'Strobe' is another very important feature, present in the 'SortSpike2' component. The 'Strobe' would produce a logical high signal every time a spike was detected. We have referred these logical high signals as 'Trig.1'from the left channel and 'Trig. 2' from right channel.

The output from the 'SortSpike2' component contained floating point time stamped spikes that satisfied threshold requirements. These were stored in memory buffers. 'SerStore' – a write only buffer; was used for this purpose. Other options like use of read and write, read-only buffers were available; however, a write-only buffer was selected, to comply with mandatory software requirements for 'SortSpike2' component [38].

Following spike detection and assigning time stamps to them it was necessary to extract these time stamp values to calculate the DA (depressor asymmetry) time difference. As described above 'Trig.1' (logical high signal) was produced with detection of every spike from the left wing; a component 'Latch' [38] was used to assign time stamp to 'Trig. 1'. The 'Latch' component takes any kind of data type as input value and a logical high as a trigger signal. In our case, we had the 'Trig. 1' as the logical high signal and the 'iTime' as input carrying the time stamp. 'iTime' (the time stamp) was latched to 'Trig. 1'.

Figure 3.6.3 presents a block diagram of the spike detection process for left wing. Floating point time stamp values of spikes from left wing EMGs were thus obtained, and firing of motor neuron from the left wing was determined. A similar process was used for spike detection on the right channel to obtain floating point time stamp values of spikes from right wing EMGs. Throughout the 'circuit', these floating point values were referred as 'T1' for the left wing and 'T2' for right wing. Figure 3.6.4 presents a block diagram for the spike detection process on right wing EMGs. Detailed circuit diagrams for the above process have been presented in Appendix D (Figures D.1 and D.2 for left wing and right wing EMG signals).

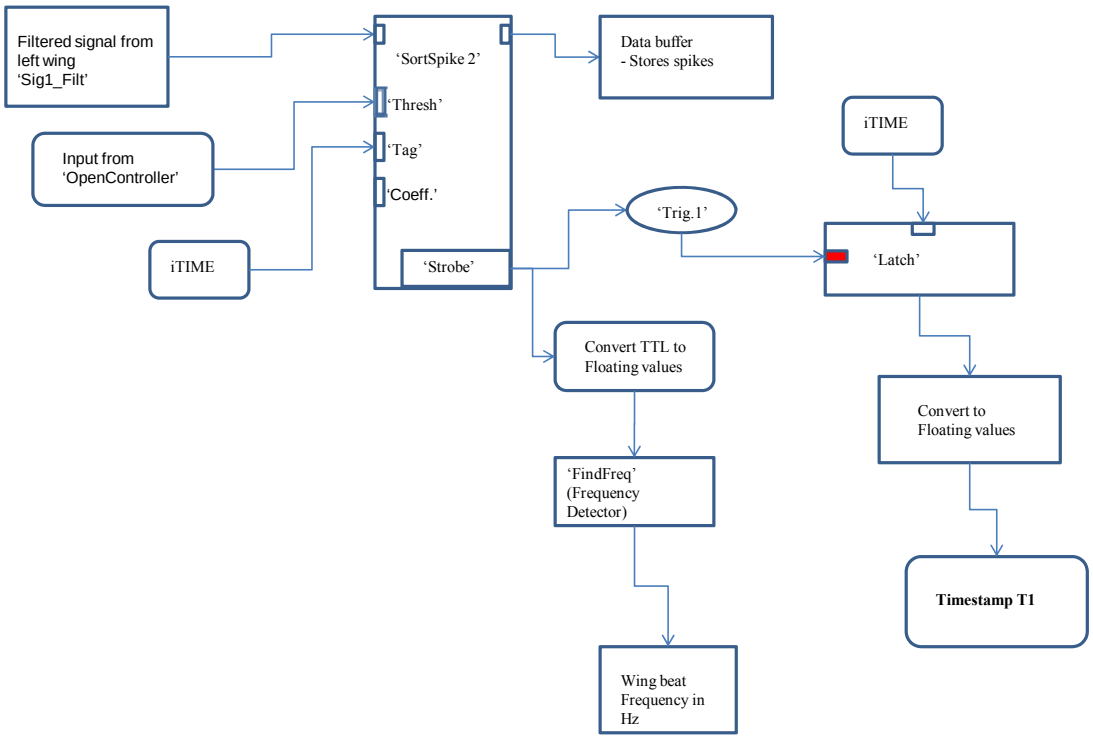

Figure 3.6.3 Spike detection of EMGs from left wing and generation of time stamps. The filtered EMG signal would be acquired by the 'SortSpike2' component. The 'Thresh' parameter received the threshold value from 'OpenController' in real-time. Based on the value of threshold spike(s) would be detected. A logical high signal referred as 'Trig. 1' was obtained from the 'Strobe' when a spike was detected. 'iTime' assigns a time stamp using a 'Latch', which is converted to floating point value 'Timestamp T1'. The output from the 'Sortspike2' component contained time stamped spikes that were stored in a data buffer.

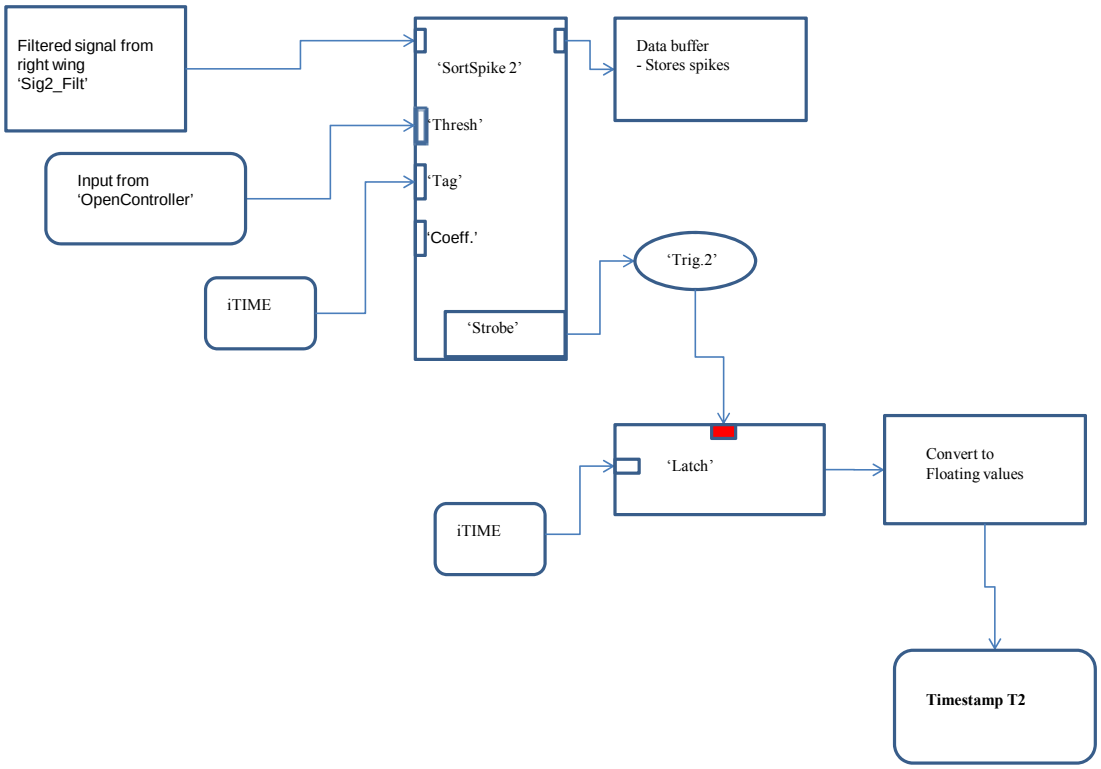

Figure 3.6.4 Spike detection of EMGs from right wing and generation of time stamps. The filtered EMG signal would be acquired by the 'SortSpike2' component. The 'Thresh' parameter received the threshold value from 'OpenController' in real-time. Based on the value of threshold the spike(s) would be detected. A logical high signal referred as 'Trig. 2' was obtained from the 'Strobe' when a spike was detected. In order to time stamp the detected spike the 'tag' parameter received 'iTime' as its input. 'iTime' assigns a time stamp using a 'Latch' which is converted to floating point value 'Timestamp T2'. The output from the 'Sortspike2' component contained time stamped spikes that were stored in a data buffer.

3.7 Wing beat frequency and voltage conversion

As described above the spike detection was done on both channels, i.e., for EMG signals acquired from left and right wing. In closed-loop experiments, one of the parameters controlling the visual stimulus for feedback relied upon detection of wing beat frequency. Thus it was imperative to perform wing beat frequency detection and convert it to analog voltage values for use in closed-loop experiments. For neurogenic fliers like locusts, firing frequency of flight motor neurons matches flight muscle and wing beat frequency. Thus, motor neuron firing frequency predicts flight speed. The 'SortSpike2' component's 'Strobe' feature would produce a logical 'high' signal (Transistor-transistor logic (TTL) signal) when a spike was detected. Hence, 'Strobe' frequency (number of times the strobe produces a logical high signal per second) can be treated as wing beat frequency. Based on this analysis, for our design a component called 'TTL2Float' was used to convert the logical high value into floating point values which were then channeled to 'FindFreq' [38] component's input parameter. The 'FindFreq' component detects the frequency of the incoming signal. As per software requirements, it was mandatory for 'FindFreq' component to have floating point data type as input in order to obtain the floating point wing beat frequency values as output. The wing beat frequency values had a range of 0 Hz ~ 25 Hz.

Wing beat frequency values between 10 Hz and 25 Hz were of particular interest as those would be the normal values observed for an airborne locust. Using a standard comparator in 'RPvdsEx' all wing beat frequency values that were above 10 Hz were detected and scaled to voltage values that were in the range of 0-5 V. Thus 10 Hz would correspond to 0 V and 25 Hz would correspond to 5 V. These analog voltage values were then obtained from the analog output

port 1 of the ‘RX5’ system. In closed-loop protocol these voltage values were used to control the forward motion of the visual scene.

A multiplexer component ‘MuxIn’ was used to control the output from the analog output port 1 of the ‘RX5’ system. The ‘MuxIn’ component received input from the comparator. If this input value was above 0 V then it would be channeled to the analog output port 1 and the observed value would be obtained; otherwise the analog output port 1 would provide 0 V output. Figures 3.7.1 and 3.7.2 present block diagrams for the process described above. In the ‘OpenController’, ‘Led Caption’ [38] feature was used to display an ON (LED GLOWING) status when wing beat frequency was between 10 ~ 25 Hz. In the ‘RPvdsEx’ ‘circuit’ a parameter tag was used to send the observed frequency value to ‘OpenController’ wherein it would be displayed using ‘Value Watch’ feature that had been named as ‘Freq_watch-10’. The detailed circuit diagram for this process has been presented in Appendix D (Figure D.2 has been reproduced as Figure D.3).

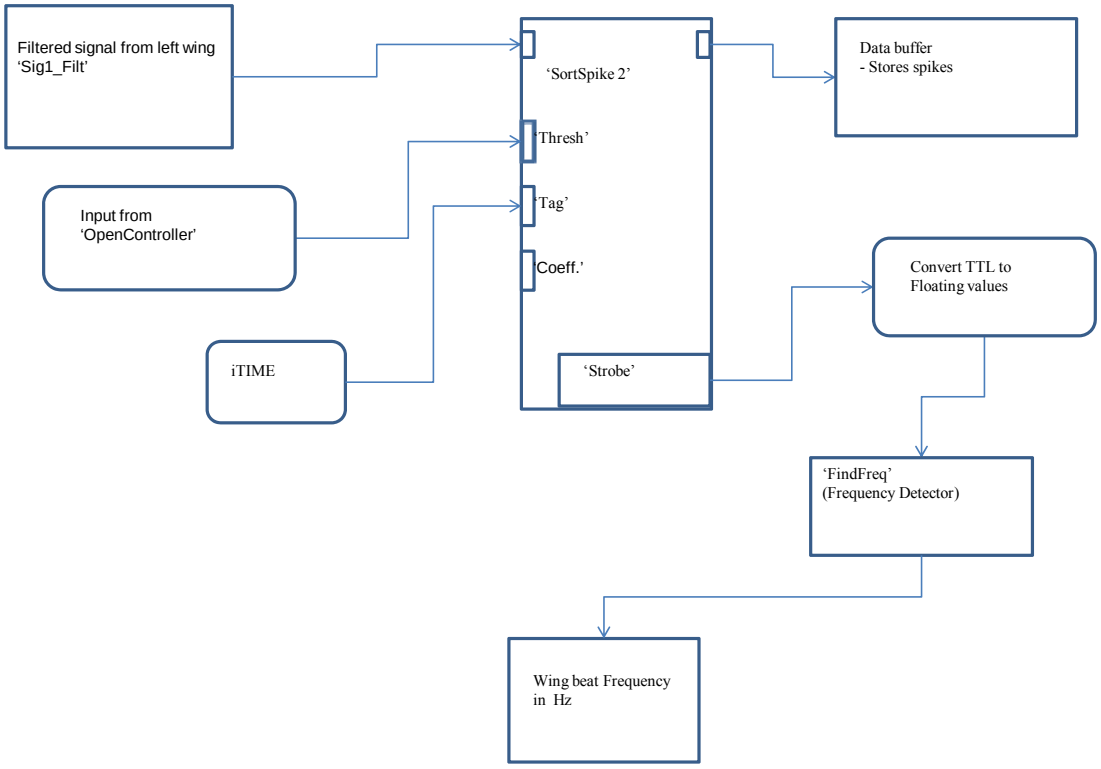

Figure 3.7.1 Spike frequency (frequency of strobe producing a logical high signal) represents wing beat frequency. Wing beat frequency was obtained using 'FindFreq' component.

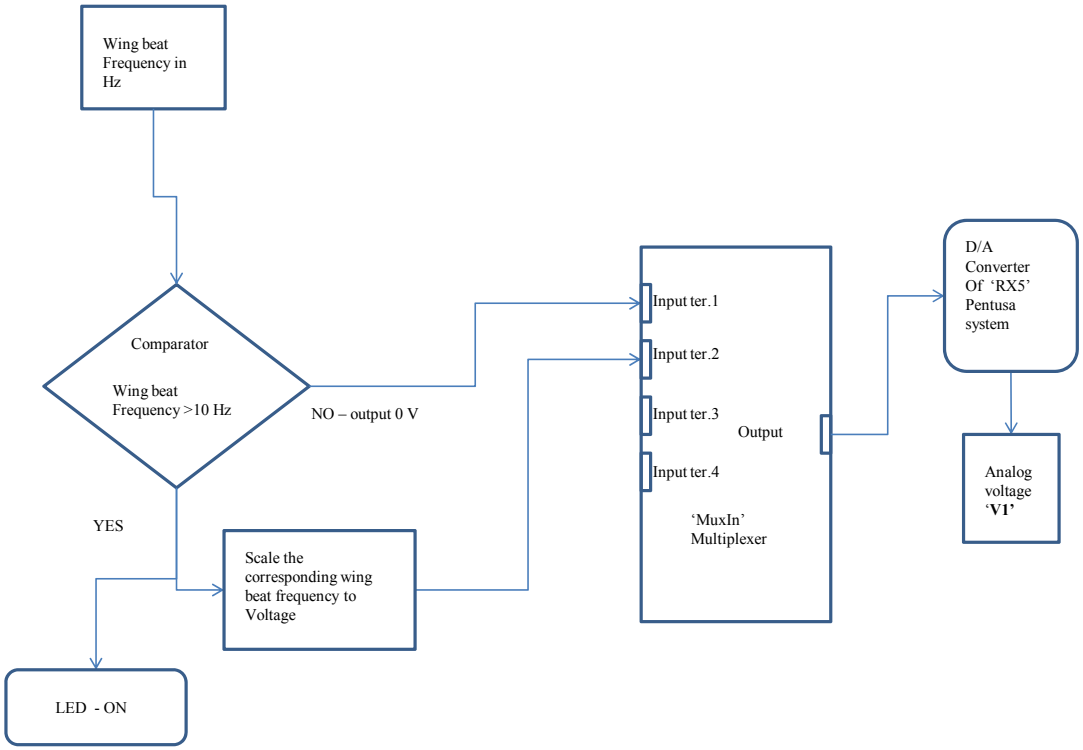

Figure 3.7.2 Using a comparator the desired range of wing beat frequency is acquired and analog voltage value V1 is obtained with the help of a D/A convertor.

3.8 Calculation of time difference between spikes

Floating point time stamp values ‘T1’ and ‘T2’ corresponding to spikes from left and right wings were obtained as described in section 3.6. We calculated the time difference between each pair of these spikes (i.e. a spike from left wing EMG and from right wing EMG). This was accomplished using the ‘Scale Add’ component in ‘RPvdsEx’ [38]. This component allows the user to add, subtract and multiply signals. As mentioned earlier, the greatest advantage of the multi-DSP system was that a signal acquired or produced from any DSP can be accessed by all other DSPs in the system. ‘T1’ and ‘T2’ values were made accessible to auxiliary DSP-IV. The ‘Scale Add’ component received ‘T1’ and ‘T2’ as inputs (floating point time stamp values) and produced ‘diff’; referred in ‘OpenController’ as ΔT (‘Delta_T’). This ‘diff’ represented the actual DA time difference. This time difference was then converted to voltage values by using ‘Scale Add’ to obtain an output voltage in the range of 0-5 V from the D/A converters of the ‘RX5’ ‘Pentusa’ system. A block diagram explaining the above process has been provided in Figure 3.8.

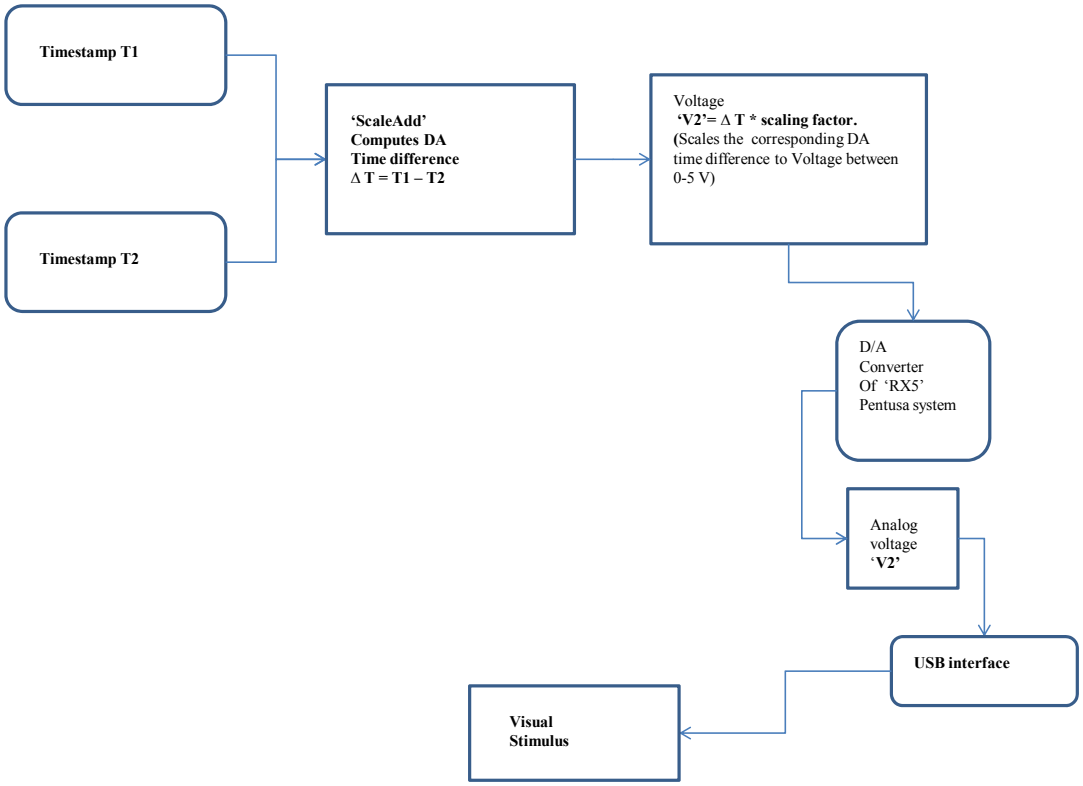

Figure 3.8 Block diagram for calculation of DA time difference and its conversion to voltage. 'Timestamp T1' and 'Timestamp T2' are obtained by assigning time stamps to spikes that have been detected. DA difference ΔT is calculated and analog voltage value V2 is obtained using a D/A convertor. These values are then acquired by a data acquisition board having a USB interface [29]. The visual stimulus described in [29] utilizes the voltage values V1 and V2 to close the feedback loop.

For closed-loop experiments, an output voltage range of 0-5 V was required. This output voltage range was intended to elicit potential left and right turns that may be made by the animal in a closed-loop and/or open-loop experiment. Thus inside the software for visual stimulus 2.5 V would be reference 0 V indicating a straight flight; and voltage values between 2.5 V to 5 V would be indicating a right turn and voltage values between 0 and 2.5 V would be indicating a left turn. A constant value of 2.5 V was added to the 'Shift' parameter [38] of the 'Scale Add' component. Thus an output of 2.5 V from the D/A would be interpreted as 0 V in the software for visual stimulus and any other value would indicate a turn.

Double spikes from left and right wings do occur during the flight of the insect (refer Figure 3.9). These may arise when the animal attempts a turn in either direction or making an attempt to steady its flight. To avoid the second spike from the same wing being detected before a spike from the other wing was accounted for, a counter was created to set a latch only at the instant after seeing one spike from both channels. It is difficult to determine whether 'T1' or 'T2' comes last, as it depends on the insect's wing movement. Hence, a logical 'OR' gate having 'T1' & 'T2' as inputs was used in the 'circuit'. The output from this 'OR' gate was connected to an 'AND' gate that also had a logical input provided by a comparator. The output of this 'AND' gate, a logical signal referred as 'latch_trig' would trigger the latch after it had detected a spike from both channels. This latch would take in the DA time difference 'diff' as input only when no double spikes were observed. This 'diff' was then channeled to a 'Scale Add' component, whose 'Shift' parameter had a constant value of 2.5V for reasons explained in the previous paragraph. In 'OpenController' a 'slider' was used to set the scaling factor in real-time that would be channeled to the processors in 'RPvdsEx' using a parameter tag.

The output from the 'Scale Add' contained scaled time differences that had been converted to voltage values in the desired range. A multiplexer component with a channel selector was used before obtaining the output voltage from the D/A. The output from the D/A was obtained using the 25 pin multiple I/O port. This 25 pin multiple I/O channel had 4 analog outputs i.e. port 1, port 2, port 3, and port 4. The DA time difference voltage value referred as 'V2' was obtained on port 4. In 'OpenController' this value of voltage was observed using the 'Value watch' and by creating a display board that was titled as 'Rotation'. This display board was updated with the parameter tag 'Rotation'-carrying the analog voltage value in the 'RPvdsEx' in real-time.

Appendix E (Figure E.1) presents the detailed circuit diagram for the process described above.

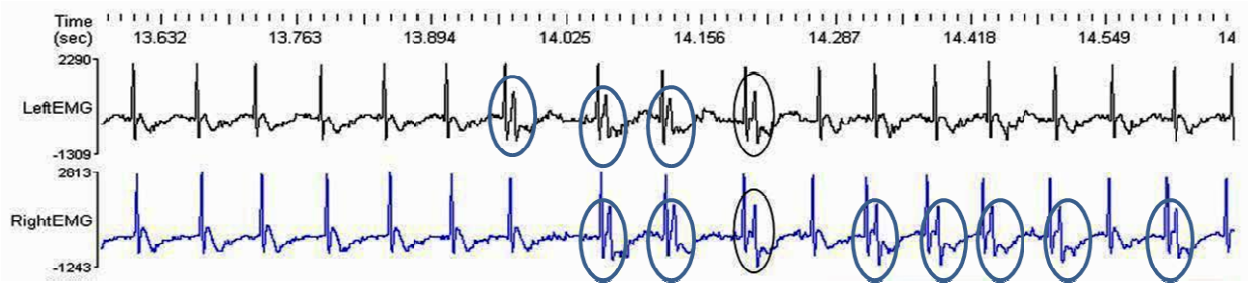

Figure 3.9 Double spikes (highlighted by ovals) resulting due to an attempted turn during insect flight.

CHAPTER 4

RESULTS

The feedback control circuit was tested with a square pulse stimulator, with wave files (.wav format) containing EMGs recorded from live animals and also with live animals. To test the circuit with recorded EMGs using wave files, EMG signals obtained from live animals, and with stimulators; we used multiplexer components that were available in the 'RPvdsEx'[38]. These allowed us to interchange between the EMGs obtained from live animals, square pulse stimulator and EMG signals in the form of wave files. These tests were performed using open-loop and closed-loop experimental paradigms. Neurophysiological data analysis software (Neuroexplorer, ver. 3.231, NEX. Technologies, Littleton, MA 01460, USA) was used to obtain Figures 4.1, 4.2, 4.3, 4.4, 4.5, 4.6, 4.7, 4.8, and 4.9. Data transferred from Neuroexplorer requires a scaling factor; the scale in all the figures (4.1-4.9) referring to voltage values (representing the DA time difference converted to voltage) needs to be multiplied by 1000 to view the voltage values in the range of 0-5 V. Owing to poor quality of EMG signals, the results obtained by using the closed-loop paradigm are discussed in Chapter 5.

4.1 Testing the feedback circuit with wave files

Pre-recorded EMG signals from locusts, stored in wave file format (.wav) were used to test the feedback control circuit for open-loop and closed-loop experiments. A step-up and step-down voltage waveform was obtained when the feedback control circuit was tested with wave files. Wave files from two animals were used to test the circuit with open-loop protocol. Figures 4.1 and 4.2 display the results obtained from two animals tested under open-loop protocol. A step-up and step-down voltage pattern was obtained. This step-up and step-down voltage waveform arises as a result of the DA. The step-up form seen in the voltage output waveform

demonstrates that m97 asymmetry shifted positively with the right muscle firing first. The fall demonstrates that m97 asymmetry shifted negatively with the left muscle firing earlier than the right muscle. These results obtained with wave files suggest that the feedback control circuit was able to acquire EMG signals, detect spikes and assign a time stamp to the event, when a motor neuron from the m97 muscles from left and right wing had fired. The circuit was also able to convert the corresponding time difference of the depressor asymmetry to voltage values. The range of the step voltage waveform was between 0-5 V.

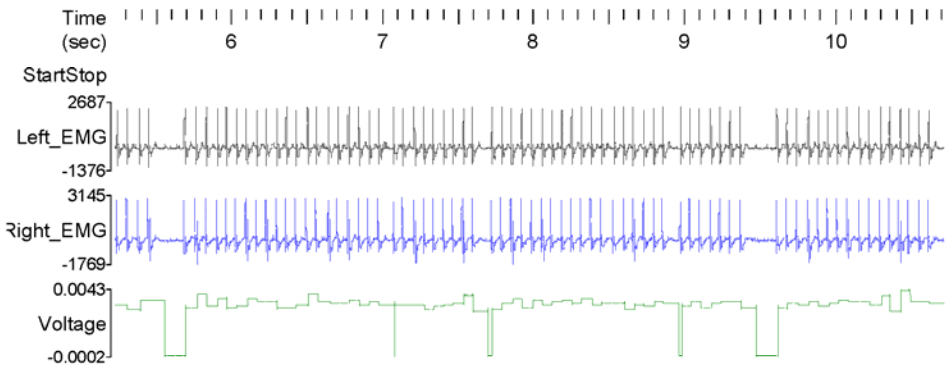

Figure 4.1 This figure shows the results obtained by testing the circuit with first set of wave files. The top trace refers to EMG from left wing, the middle trace - EMG from right wing. The step-up and step-down voltage waveform (bottom trace) represents the depressor asymmetry.

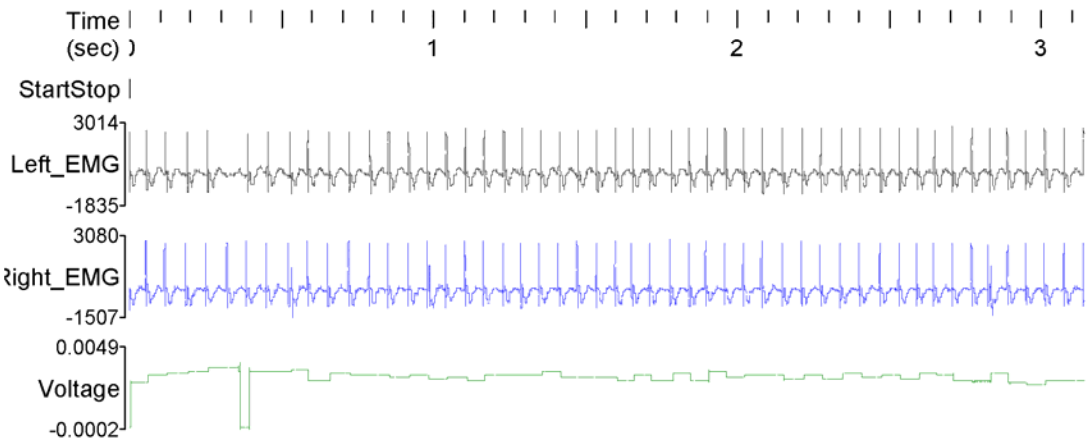

Figure 4.2 This figure shows the results obtained by testing the circuit with a second set of wave files. The top trace refers to EMG from left wing, the middle trace - EMG from right wing. The step-up and step-down voltage waveform (bottom trace) represents the depressor asymmetry.

4.2 Testing the feedback circuit with Locusts:

The results obtained by testing the feedback circuit with locusts have been split in two subsections:

A) Testing the feedback control circuit with locusts in an open-loop paradigm.

    1) Response to a stimulus presented to the locust from the left

    2) Response to a stimulus presented to the locust from the right.

Responses of the locust to a stimulus presented from the right and left were tested for one animal (animal 2) only.

B) Testing the feedback control circuit with locusts in a closed-loop paradigm

4.2.1 Testing the feedback control circuit with locusts in an open-loop paradigm

The feedback control circuit was tested with locusts to convert the DA time difference to voltage values in real-time. In the open-loop experimental protocol EMG signals were acquired in real-time and processed by the feedback control circuit. A stimulus may be presented in the open-loop experiment to test the performance of the circuit. The open-loop experiment lacks a feedback loop. In the context of the feedback control circuit, the circuit's performance is tested in terms of its ability to convert DA to voltage values. The stimulus that may be presented in the experiment will not be controlled by the animal. The feedback control circuit was able to detect the DA time difference and produce a step-up and step-down voltage waveform similar to that observed when testing the circuit with wave files.

Figures 4.3, 4.4, and 4.5 present results obtained by testing the feedback control circuit using the open-loop paradigm (without presentation of stimulus) with 3 different locusts tagged as animal 1, animal 3, animal 4. A puff of air was blown from the anterior of the locust to initiate flight of the insect. Muscle activity was recorded with the commencement of flight. These

figures present the EMG traces acquired from left and right wing and the corresponding voltage output. The top two traces depict the EMGs acquired from (left and right wing), and the bottom trace represents the voltage waveform resulting from the DA.

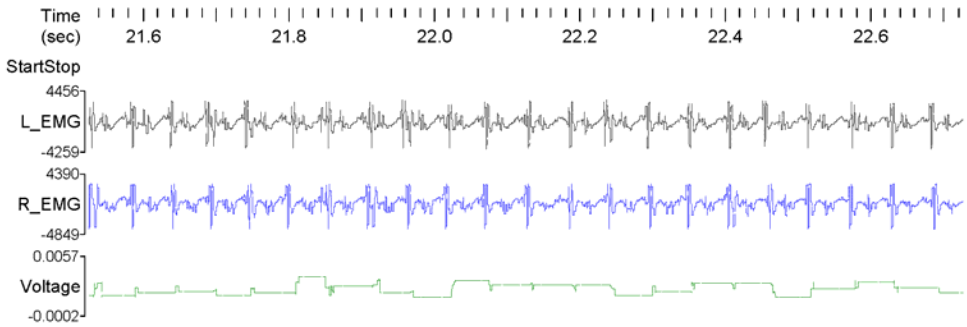

Figure 4.3 Results from open-loop experiment. EMG signals and voltage waveforms acquired from animal 1. The top trace refers to EMG from left wing, the middle trace - EMG from right wing. Step-up and step-down voltage pattern (bottom trace) can be observed arising from DA time difference. No stimulus was presented during this experimental trial.

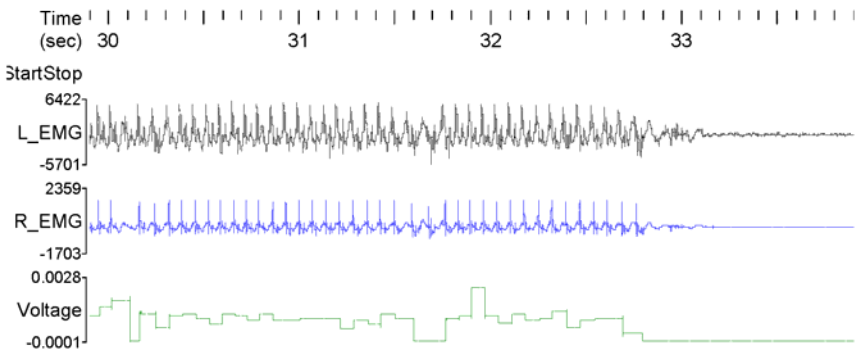

Figure 4.4 Results from open-loop experiment. EMG signals and voltage wave forms acquired from animal 3. The top trace refers to EMG from left wing, the middle trace - EMG from right wing. Step-up and step-down voltage pattern (bottom trace) can be observed arising from DA time difference. No stimulus was presented during this experimental trial.

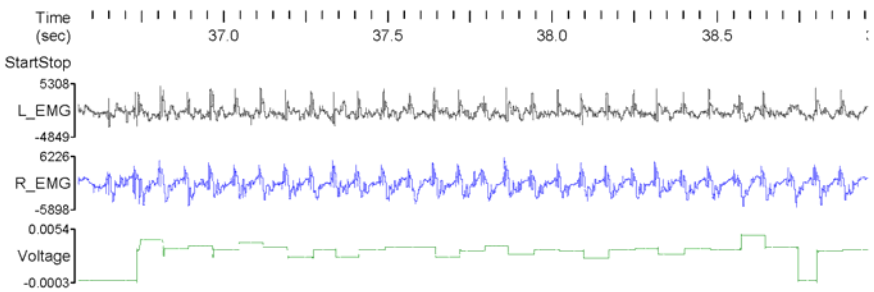

Figure 4.5 Results from open-loop experiment. EMG signals and voltage waveforms acquired from animal 4. The top trace refers to EMG from left wing, the middle trace - EMG from right wing. Step-up and step-down voltage pattern (bottom trace) can be observed arising from DA time difference. The EMG waveforms in the present figure appear to be different due to error in the placement of electrodes. No stimulus was presented during this experimental trial.

4.2.1.1 Response to a stimulus presented to the locust from right

Right forewing depressor muscles advanced in timing when the stimulus was presented from the right during an open-loop experiment.

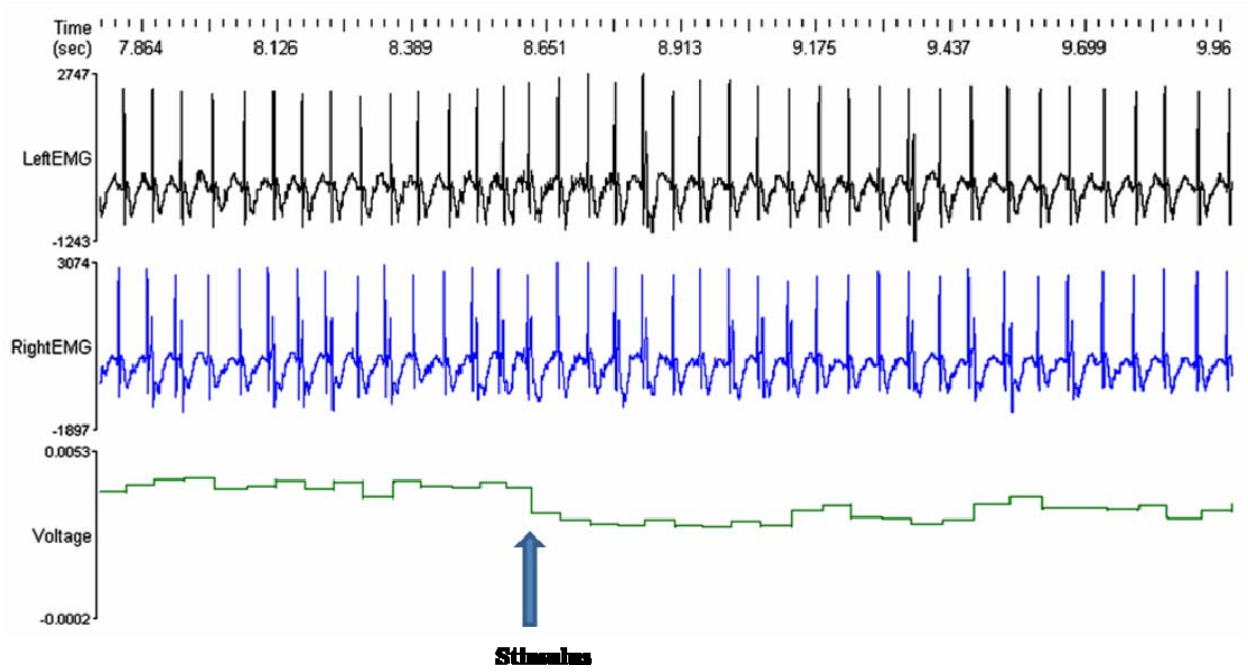

Figure 4.6 EMG signals and voltage waveforms acquired from animal 2. The top trace refers to EMG from left wing, the middle trace - EMG from right wing. Step-up and step-down voltage pattern (bottom trace) can be observed arising from DA time difference. The step-up and step-down voltage waveform also highlights the response of the animal when presented with a stimulus from the right, (marked by a drop in voltage values). The arrow indicates the approximate position of collision of stimulus with the locust. The locust's intent to avoid collision with the identified stimulus can be confirmed by the decreasing voltage values observed after the arrow. The decreasing voltage values indicate a turning maneuver by the locust.

The locust was able to identify the stimulus and attempted a left turn. The decreasing voltage values (after the arrow) observed in Figure 4.6 clearly indicate that the locust attempted to avoid the collision with the stimulus by initiating a left turn. These voltage values are arising

from the conversion of DA time difference. The approximate time and position by which the stimulus would have collided with locust is indicated by the arrow.

4.2.1.2 Response to a stimulus presented to the locust from left

Left forewing depressor muscles advanced in timing when the stimulus was presented from the left during an open-loop experiment.

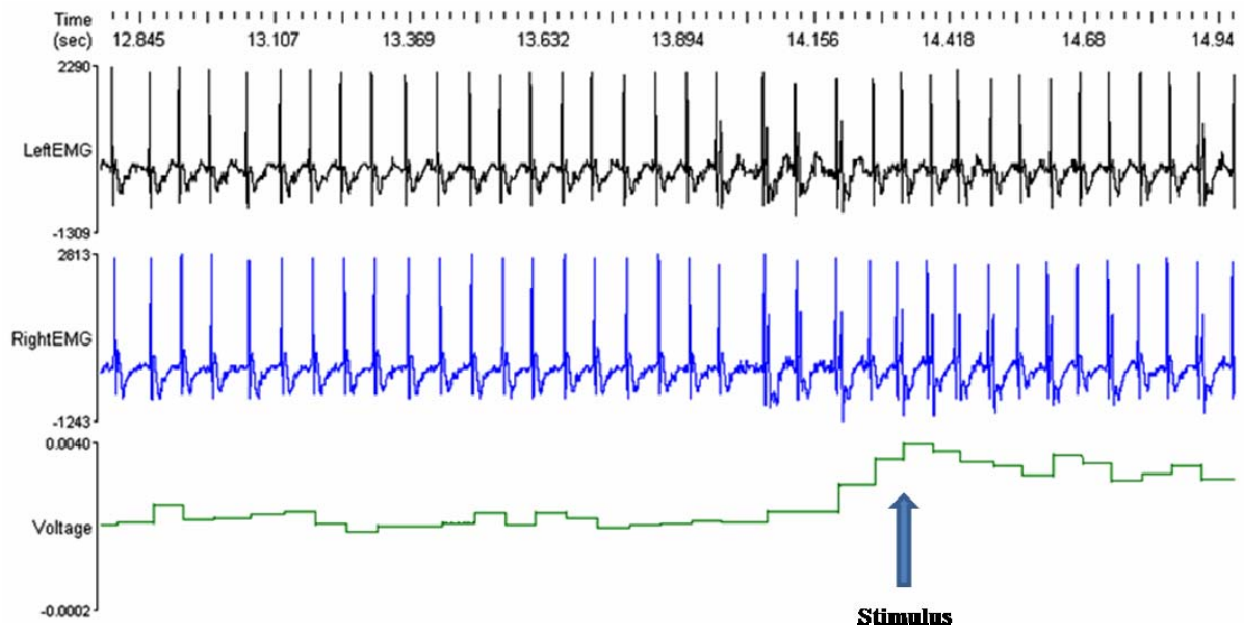

Figure 4.7 EMG signals and voltage waveforms acquired from animal 2. The top trace refers to EMG from left wing, the middle trace - EMG from right wing. Step-up and step-down voltage pattern (bottom trace) can be observed arising from DA time difference. The step-up and step-down voltage wave form also highlights the response of the animal when presented with a stimulus from the left, (marked by a rise in voltage values). The arrow indicates the approximate position of collision of stimulus with the locust. The locust's intent to avoid collision with the identified stimulus can be confirmed by the increasing voltage values observed before the arrow. The increasing voltage values indicate a turning maneuver by the locust.

The locust was able to identify the stimulus and attempted a right turn. The increasing voltage values (before the arrow) observed in Figure 4.7 clearly indicate that the locust attempted to avoid the collision with the stimulus by initiating a right turn. These voltage values are arising

from the conversion of DA time difference. The approximate time and position by which the stimulus would have collided with locust is indicated by the arrow.

Figures 4.6 and 4.7 show traces of EMG signals acquired from left and right m97 muscles and the corresponding time difference of the depressor asymmetry converted to voltage. This step voltage waveform had a range of 0-5V. Depressor asymmetry when positive would initiate the right muscle to fire earlier than the one from the left wing. This resulted into a step-up (rising) shape of the voltage waveform. DA when negative would initiate the muscle from the left wing to fire earlier than the one from the right wing thus resulting into a step-down (falling) shape of the voltage waveform. The feedback control circuit in the open-loop paradigm was thus able to detect the event when a spike had occurred, calculate the DA time difference and convert it to voltage values.

The m97 depressor muscle is also known to fire more than one spike per burst (highlighted circles in Figure 4.8). These double spikes were observed during both open and closed-loop experiments. To avoid the problem of a doublet (double) or triplet (triple) spikes being detected and to identify a clear spike satisfying the threshold values set by the user, a counter to identify the dual / triple spike was set up.

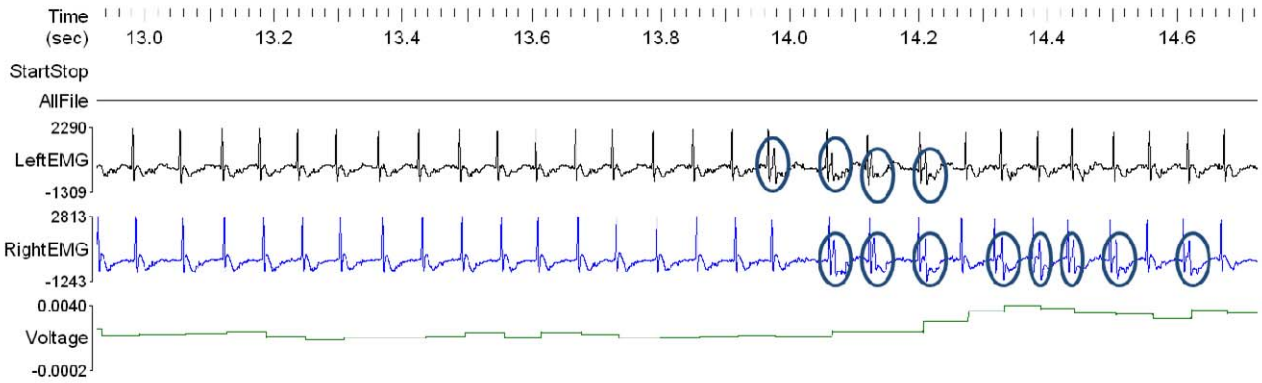

Figure 4.8 Double spikes observed in EMG signals acquired from animal 2. Highlighted circles depict the double spikes. The top trace represents signal from left wing, the middle trace – from the right wing, the bottom trace represents the voltage waveform arising from the DA time difference. The step-up and step- down voltage pattern arising from DA time difference is also visible.

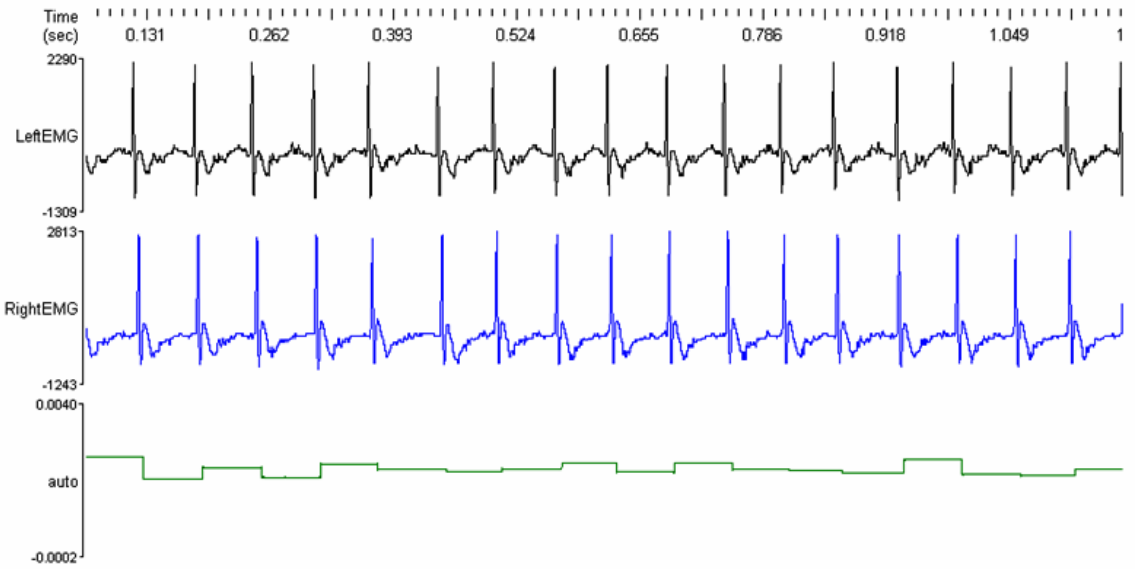

Figure 4.9 Plot of EMG latency against time. The EMG signals and voltage waveforms were acquired from animal 2. The top trace refers to EMG from left wing, the middle trace - EMG from right wing. 'Auto' represents the step-up and step-down voltage pattern arising from DA time difference.

4.2.2 Testing the feedback control circuit with locusts in a closed-loop paradigm

Data was recorded from 5 animals. In the closed-loop paradigm the feedback control circuit made use of the wing beat frequency and the DA time difference to close the feedback loop. The output from the feedback control circuit consisted of 2 channels of analog voltage V1 and V2. V1 and V2 represented frequency converted to voltage and DA converted to voltage respectively. Stimulus designed by Arkles [29] was used for closed-loop experiments. Arkles [29] has described the development of a data acquisition board that mapped the wing beat frequency represented by analog voltage V1 produced by the feedback control circuit onto

forward velocity and the DA between the left and the right onto angular velocity represented by analog voltage V2 using an analog to digital converter. This gave the animal complete (velocity and yaw) control of the visual environment developed and described by Arkles in [29]. A complete description of the data acquisition board and the schematics are beyond the scope of this thesis work.

The results pertaining to the closed-loop paradigm are presented in the Chapter 5 – Discussion, in the form of plots of EMG signals and the corresponding wave voltage waveforms (Figures 5.1 - 5.2) representing spike time difference.

4.3 Summary of Results:

The results of both the open-loop and closed-loop experiments indicate that the feedback control circuit was able to detect the DA time difference and convert it to analog voltage values. The circuit was also able to avoid the double spikes and identify the correct pair of firing motor neuron units. In the case of the open-loop experiment where a stimulus was presented invoking the insect flight the step-up and step-down voltage obtained clearly gave us an indication of the motor neuron unit firing from a specific wing. The results obtained from the closed-loop experiments indicate that the locust was able to control its flight in the visual environment by making use of the DA time difference and the wing beat frequency that had been converted to voltage. The feedback control circuit was able to address two major issues that led to its development: a) making use of DA time difference to control visual field and b) it no longer relied on abdomen position as a tool to provide feedback and control visual stimulus.

CHAPTER 5

DISCUSSION

The results obtained by testing the feedback control circuit both in open-loop and closed-loop paradigm suggest that it was able to meet its objectives. Testing the circuit in open-loop paradigm by presenting a stimulus and thereby invoking the flight of the locust, it was observed that the circuit was able to detect the DA time difference and convert it to voltage values. During an intentional turn to the right, the right forewing is more depressed than the left during the down stroke [28]. The performance of the circuit concurs with this biological observation. It has been reported by Shoemaker and Robertson [28] that *"bulk shifts"* in muscle activities may be required to produce these DA. During the turning maneuvers exhibited in left and right directions the timing of contracting muscles controlling the stroke reversal must have been modified. These *"bulk shifts"* have been related to the advancement of timing of all forewing depressor muscles compared to other muscles [28]. It is also known that these timing differences in basalar muscles are capable of invoking wing movements [32]. This is evident in the closed-loop experiments wherein the shifting of the 'Cube' in the direction of the turn can be observed (refer screen captures obtained from 5 different animals). We also observed that depressor asymmetry was positive for the step rise (right muscle firing first) and was negative for fall (left muscle firing first). Moreover, the muscle on the inside of the intended turn often produced two spikes per burst while that on the outside showed either no change or a decrease in the number of spikes per burst (Figure 4.8 reproduced below).

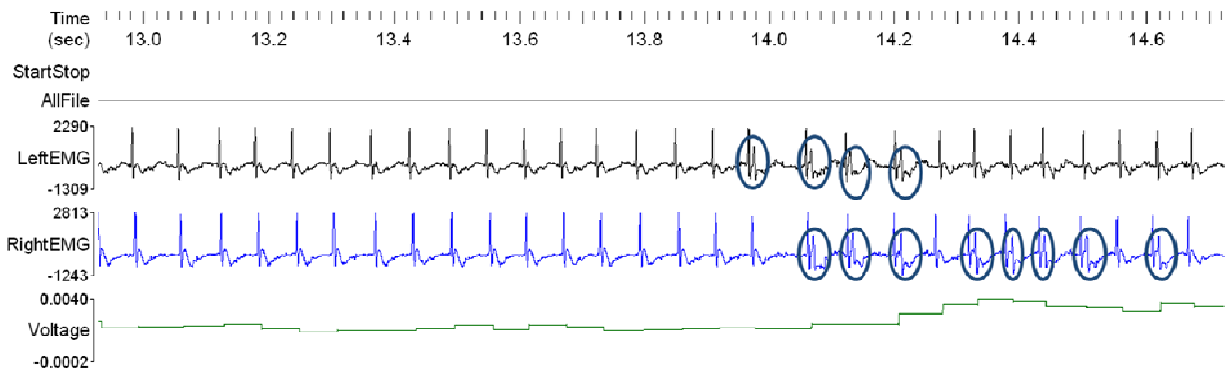

Figure 4.8 Double spikes observed in EMG signals acquired from animal 2. Highlighted circles depict the double spikes. The top trace represents signal from left wing, the middle trace – from the right wing, the bottom trace represents the voltage waveform arising from the DA time difference. The step-up and step- down voltage pattern arising from DA time difference is also visible.

When a stimulus was presented during an open-loop experiment an increase in the wing beat frequency (from approximately 20 Hz to 25 Hz) along with a sharp rise in the output voltage values (Figures 4.6 and 4.7) was observed. This is consistent with previous findings [9]. The turning behaviors exhibited by the locust also exhibited a sudden rise in voltage value and wing beat frequency which agrees with the findings of Dawson et al. [13].

The control of the visual stimulus by the locust, during the closed-loop experiment can be considered as an example of 'positive feedback' as in a positive feedback system the system responds in the same direction as the perturbation.

We were not able to obtain good quality EMG signals in the closed-loop experimental paradigm. As a result, plots of EMG signals and the corresponding voltage waveforms (Figures 5.1-5.2) representing spike time difference have been presented here for 2 animals only. In spite of this drawback, we observed that animals were able to control the orientation of the 'Cube' in the virtual environment (refer to screen capture obtained from five animals Figures 5.3-5.7).

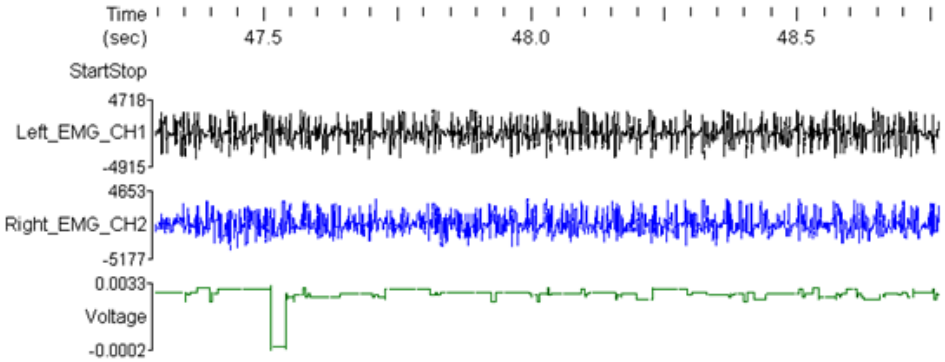

Figure 5.1 Result from closed-loop experiment. EMG signals and voltage waveforms acquired from animal 4 during closed-loop experiment. Step-up and step-down voltage pattern can be observed arising from DA time difference.

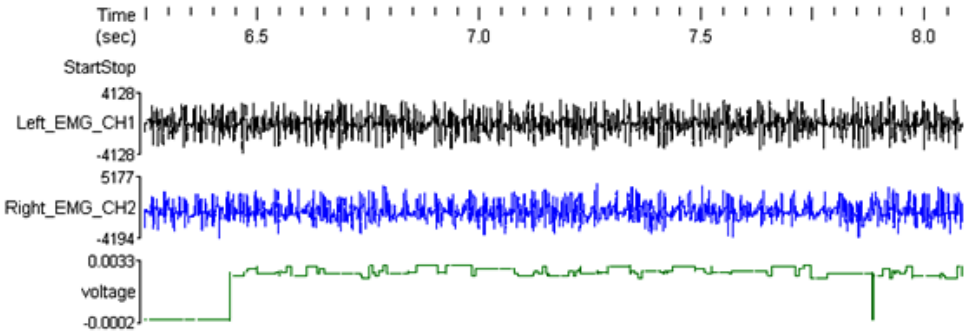

Figure 5.2 Result from closed-loop experiment. EMG signals and voltage waveforms acquired from animal 5 during closed-loop experiment. Step-up and step-down voltage pattern can be observed arising from DA time difference.

By performing further closed-loop experiments, comparing the presented closed-loop stimulus and the locust's EMG activity, the circuit's performance can be verified and an insight into the reliability of using DA time difference as a feedback parameter in understanding of the locust's flight behavior can be gained.

5.1 Screen capture results

Screen capture images of the video evidence from 5 animals used in closed-loop experiments have been presented here showing how the animal was able to control the visual scene based on the voltage values V1 and V2. The screen capture images suggest that the locust was able to control the orientation of the 'Cube'. The 'Cube' when approaching the locust was identified by it as a stimulus and hence it would prompt a turning maneuver in either the left or right direction.

5.1.1 Screen captures from animal # 1

The set of images (Figure 5.3 A to F) are the screen captures obtained from animal 1 during a closed-loop experiment. Initially the object would appear facing the animal and would move only when the animal commences its flight. The screen captures were taken at an instant of time when the animal would have been able to move the object towards its left or right direction. Parameters like the size of the object would be controlled by the animal itself. Analog voltage values V1 and V2 representing wing beat frequency and DA values would be used to control the parameters of the object. Screen capture A (at 00.24 seconds) indicates that object was initially smaller in size and then gradually grew as the animal flew for a longer period. Screen capture F (at 9.13 seconds) indicates that the object appears to be on the left side of the animal and is larger in size.

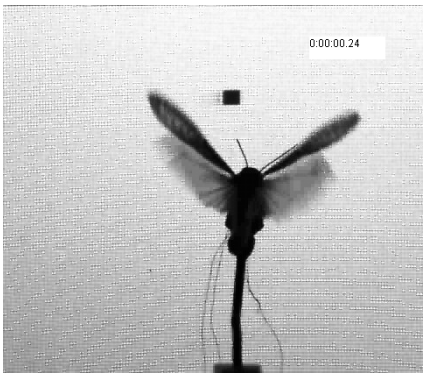

A (time 0:00:00.24)

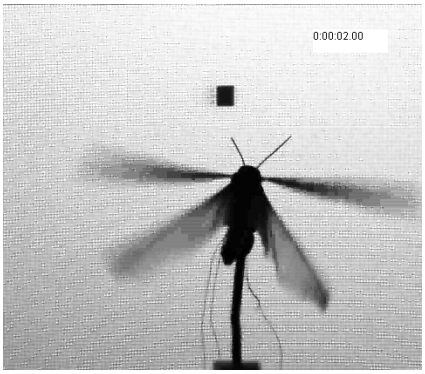

B (time 0:00:02.00)

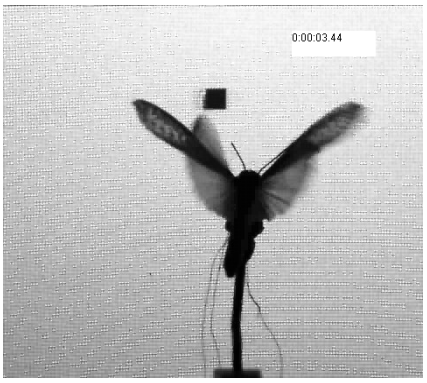

C (time 0:00:03.44)

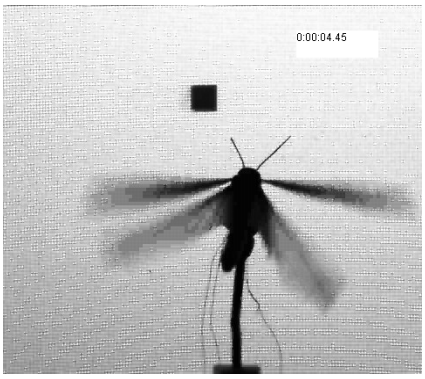

D (time 0:00:04.45)

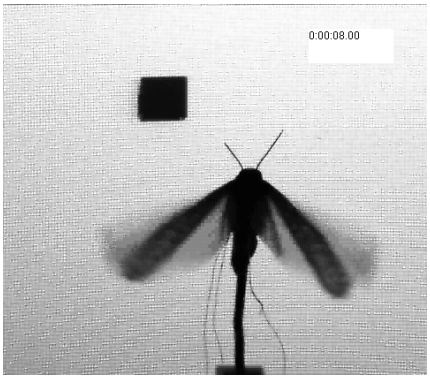

E (time 0:00:08.00)

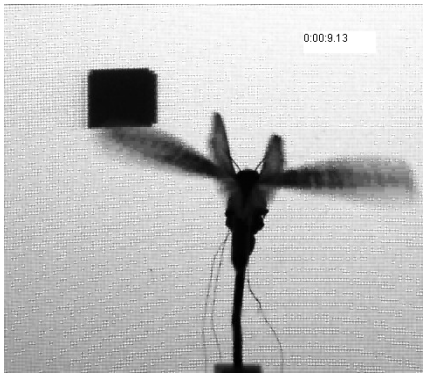

F (time 0:00:09.13)

Figure 5.3 Screen captures (A-F) obtained from animal 1 during a closed-loop experiment.

5.1.2 Screen captures from Animal # 2

The set of images (Figure 5.4 A to D) are the screen captures obtained from animal 2 during a closed-loop experiment. The screen captures were taken at an instant of time when the animal would have been able to move the object towards its left or right direction. Parameters like the size of the object would be controlled by the animal itself. Analog voltage values V1 and V2 representing wing beat frequency and DA values would be used to control the parameters of the object. Screen capture A (at 1.34 seconds) indicates that object was initially smaller in size and then gradually grew as the animal flew for a longer period. Screen capture D (at 15.56 seconds) indicates that the object appears to have shifted to the left of the animal and is larger in size.

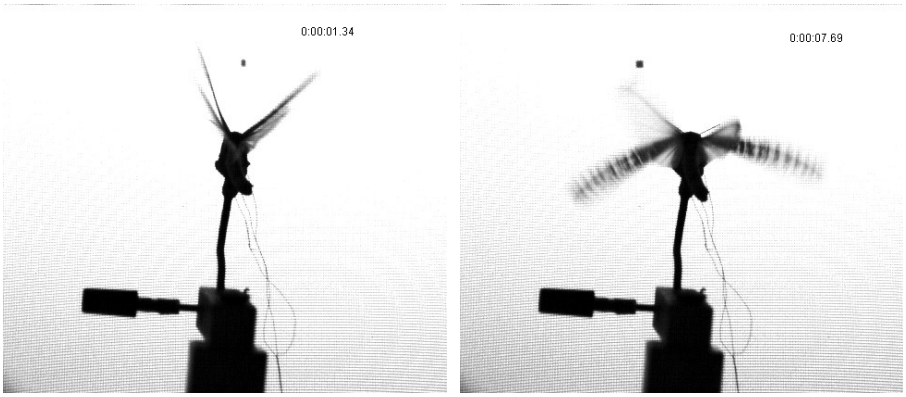

A (time 0:00:01.34) B (time 0:00:07.69)

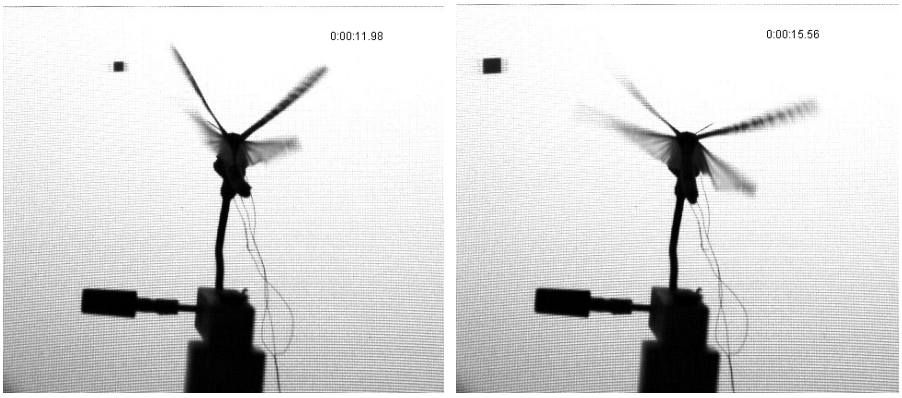

C (time 0:00:11.98) D (time 0:00:15.56)

Figure 5.4 Screen captures (A-D) obtained from animal 2 during a closed-loop experiment.

5.1.3 Screen captures from Animal # 3

The set of images (Figure 5.5 A to D) are the screen captures obtained from animal 3 during a closed-loop experiment. The screen captures were taken at an instant of time when the animal would have been able to move the object towards its left or right direction. Parameters like the size of the object would be controlled by the animal itself. Analog voltage values V1 and V2 representing wing beat frequency and DA values would be used to control the parameters of the object. Screen capture B indicates that object, initially smaller in size and being controlled by the animal appears towards its right. Screen capture D indicates that the object has shifted and now appears to be on the left side of the animal and is also larger in size.

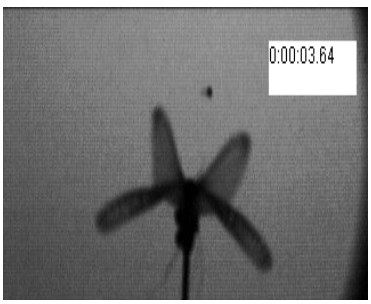

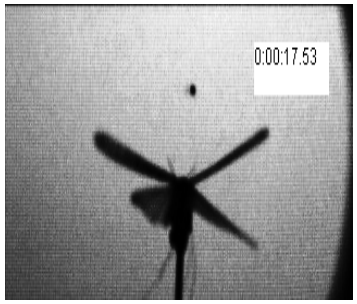

A (time 0:00:03.64) B (time 0:00:17.53)

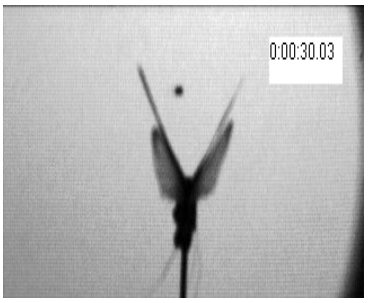

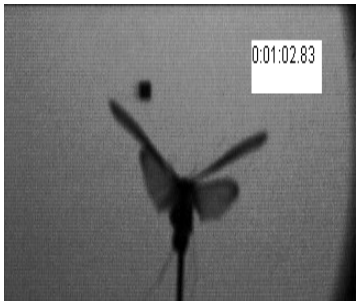

C (time 0:00:30.03) D (time 0:01:02.83)

Figure 5.5 Screen captures (A-D) obtained from animal 3 during a closed-loop experiment.

5.1.4 Screen captures from Animal # 4

The set of images (Figure 5.6 A to F) are the screen captures obtained from animal 4 during a closed-loop experiment. The screen captures were taken at an instant of time when the animal would have been able to move the object towards its left or right direction. Parameters like the size of the object would be controlled by the animal itself. Analog voltage values V1 and V2 representing wing beat frequency and DA values would be used to control the parameters of the object. Screen capture A indicates that object was initially smaller in size and then gradually grew as the animal flew for a longer period. Screen capture B indicates that the object appears to be on the left side of the animal and is also larger in size. Screen capture C indicates that the object appears to be facing the animal as the animal may have intended to turn. Screen capture D

(at 4.42 seconds), E (at 8.47 seconds) and F (at 13.70 seconds) indicate that the object appears to have shifted to the left side of the animal.

A (time 0:00:00.70)

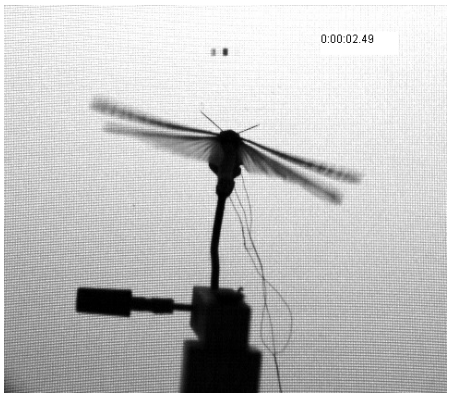

B (time 0:00:02.49)

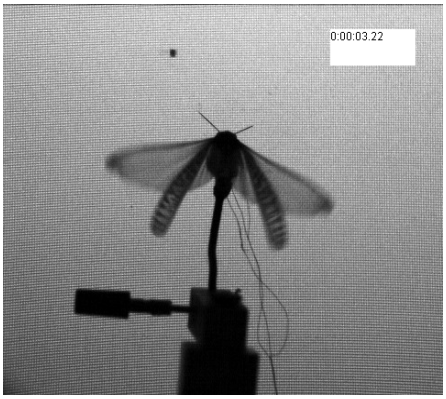

C (time 0:00:03.29)

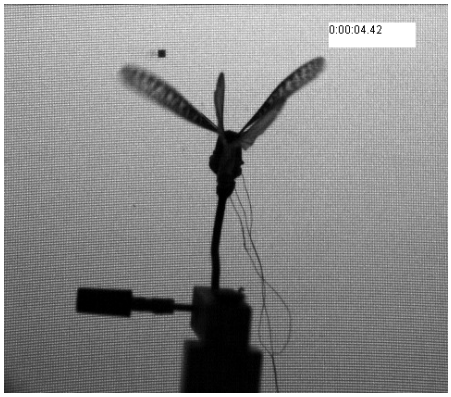

D (time 0:00:04.42)

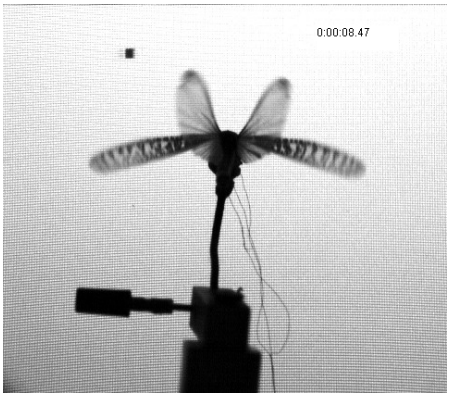

E(time 0:00:08.47)

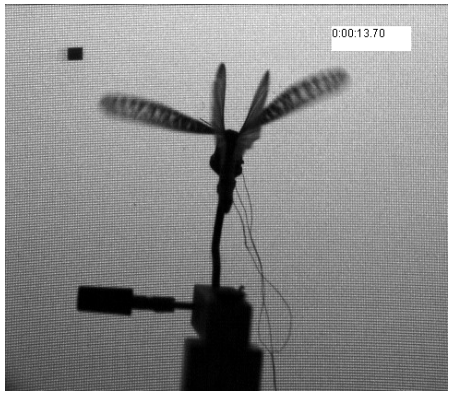

F(time 0:00:13.70)

Figure 5.6 Screen captures (A-F) obtained from animal 4 during a closed-loop experiment.

5.1.5 Screen captures from Animal # 5

The set of images (Figure 5.7 A to E) are the screen captures obtained from animal 5 during a closed-loop experiment. The screen captures were taken at an instant of time when the animal would have been able to move the object towards its left or right direction. Parameters like the size of the object would be controlled by the animal itself. Analog voltage values V1 and V2 representing wing beat frequency and DA values would be used to control the parameters of the object. Screen capture A (at 6.11 seconds) indicates that object was initially smaller in size and was facing the animal. Screen capture B indicates that the object appears to have been shifted towards the left side of the animal and is also larger in size. Screen capture E (at 12.57 seconds) indicates that the object appears to be larger in size and also on the left side of the animal.

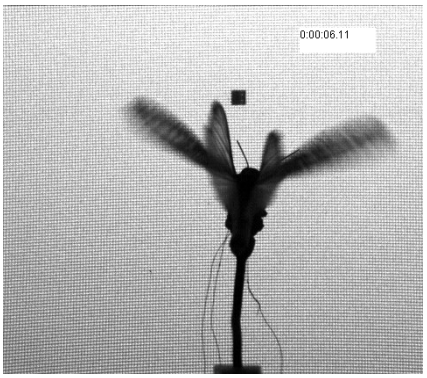

A (time 0:00:06.11)

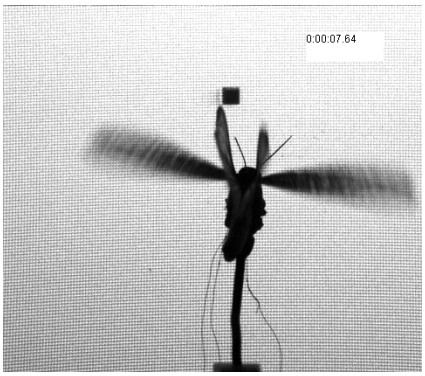

B (time 0:00:07.64)

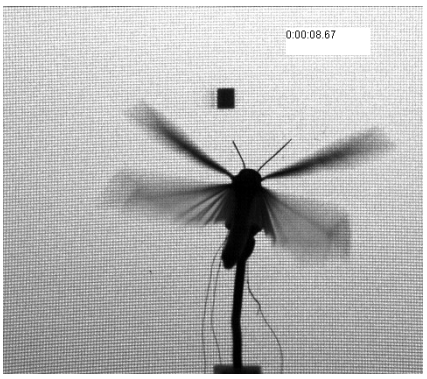

C (time 0:00:08.67)

D (time 0:00:10.91)

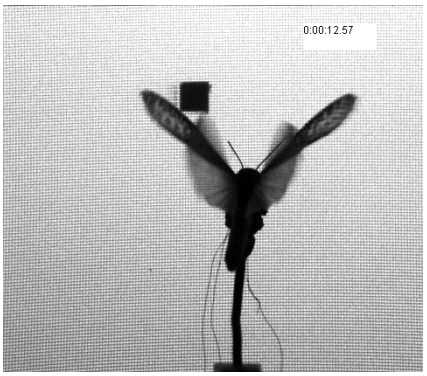

E (time 0:00:12.57)

Figure 5.7 Screen captures (A-E) obtained from animal 5 during a closed-loop experiment.

The sequences of images presented above are from five animals. The object, a square box in 2 dimension (‘Cube’ in 3-D), described by Arkles in [29] would appear at the centre of the dome once the insect started flying. The size of the square box and its orientation were completely controlled by the insect. These parameters were proportional to the voltage values obtained by converting the DA time difference and the wing beat frequency.

It can be seen from the screen captures obtained from 5 animals and the corresponding traces of EMG and voltages waveform (Figures 5.1-5.2 from 2 animals only) presented here, that the locust was able to control the orientation of the square box. A right turn by the locust would move the ‘Cube’ towards left and vice-versa. The ‘Cube’ when approaching to the locust was

identified by it as a stimulus and hence it would prompt a turning maneuver in either left or right direction and would disappear from the visual field of the locust.

5.2 Comparison with other methods using the concept of feedback control.

5.2.1 Comparison with other feedback approaches using locusts as a model

Möhl [7] used a flight simulator and feedback control approach to study the locust flight by calculating the time difference between the firing of the motor neuron(s) in the m129 muscles. This time difference was fed back to a *"yaw angle stimulus device"* to control the yaw angle with which the locust would fly in the air stream of the wind tunnel [7]. In this closed-loop set-up, the locusts were able to adjust the timing of m129 muscles and align their body axis correctly. Möhl suggested that the insect possessed a memory feature that would coordinate the flight muscle activity both in open-loop and closed-loop experiments. In his approach, the time difference between the muscle action potential was compared to a reference value determined by the experimenter, and a deviation from the reference value would control the yaw stimulus. In comparison to the approach adopted by Möhl [7], no reference values were used by the method presented in this thesis work; as it was intended that the animal should have complete control of the stimulus in real-time. That is, in closed-loop conditions, if it decided to turn right then a corresponding rise in voltage coupled with increase in wing beat frequency should be observed. The results obtained using the method presented in the thesis work was as expected, and hence it can be suggested that the memory feature suggested by Möhl can also be extended to the m97 - first basalar depressor muscles. Möhl observed a specific motor pattern arising due to timing of m129 muscles. Compared to Möhl's approach a different set of muscles were used in this research work, however, a similar motor pattern arising due to the timing of m97 muscles was observed. The feedback control 'circuit' demonstrated a robust performance by identifying the

coordination of depressor muscle activity which is part of the locust's in-built control circuit allowing it to also control the apparent position of the 'Cube'.

We have demonstrated that the feedback control circuit was able to identify the asymmetry in the timing of the muscle potentials (EMG) from the m97 muscles and convert it to voltage values to control the visual stimulus - 'Cube'. Failure to do so, would have given us a fixed position of the 'Cube' as it would not have been able to identify and avoid the potential collision with the object [39].

To understand steering behaviors in locusts, Robert and Rowell [5,6] have presented a flight simulator design and a closed-loop experimental protocol, where the yaw torque produced by locust was used to control the visual landscape. The *'torque meter'* as described by Robert and Rowell [5] would control the angular velocity of the visual environment being changed. In comparison to their method, the method presented in this thesis work, gives the animal complete control of its visual field and thus may help to understand the steering behaviors in a better way given the fact that we are recording from forewing depressor muscles that play a significant role in steering behaviors. The approach used by Robert and Rowell [5] also had a limitation that the torque produced by the animal in a given direction needed to force the visual field to rotate in the opposite direction. The method used in this thesis work avoids this limitation, as DA either positive or negative would automatically control the 'Cube' (visual stimulus) in corresponding direction indicating a turn. Also, Robert and Rowell had not utilized electromyographic activity as an input to the *'torque meter'*. Our system depending on electromyographic activity for feedback control presents a good example of a positive feedback system. It has been suggested by Kutsch [40] that motor output modification is more prominent in the case of forewing muscles as compared to hindwing muscles, as the former are responsible for flight maneuvers

while the latter serve to power the flight. The major advantage of the presented technique is the novel approach to associate and use time difference in muscle activity to understand complex flight parameters. Balint and Dickinson [23] have suggested that change or activation of pattern in the motor neuron unit(s) results in modification of muscle action i.e. production of muscle contraction. This contraction in turn gives rise to a change in the shape of sclerite; thus the muscle acting as an output transducer triggers a change in wing movements. The novel approach of using m97 DA for feedback control concurs with the suggestions of Balint and Dickinson [23].

5.2.2 Comparison with other feedback approaches using fruitfly as species

The goal of the method and design of the feedback control system presented here was to replace the abdomen position sensor which relied on a photodiode based sensor. This system can also be used for other biological species like fruitfly and hawkmoth. A feedback control system, which used an optical flight simulator utilizing spike frequencies observed in steering muscles responsible for flight as control signals, was presented by Götz [24,25]. The new approach presented by us for investigating locust flight control may be used to study fruitfly flight kinematics. It may be possible to obtain better results compared to the system presented by Götz [24,25], due to the fact that we are recording directly from the flight muscles. It has been reported by Balint and Dickinson [23] that for a blowfly, a strong correlation can be observed in the timing of each spike of the basalar muscle coupled with change in the deviation of the stroke plane during a downward wing stroke. A better understanding of blowfly flight dynamics in a closed-loop system [41] may be obtained using the spike time difference method and design proposed in this thesis work.

5.3 Possible applications

The method and design presented here gives us the flexibility to use it to process muscle action potential activity from other sets of flight muscles like m129, m98, m127, and m99 involved in locust flight. These muscles are known to exhibit DA though not as prominent as observed in m97. The basic design for processing signals from those muscles would remain the same; however the threshold parameters would require adjustment in real-time as the spikes produced by the motoneurons from these muscles may be of variable amplitude. This would require changes in the sort code of the 'SortSpike2' [38] component for both channels.

5.3.1 Replacement of abdomen position sensor for investigating moth flight

Kammer and Nachtigall [8] have suggested that moths exhibit diverse flight maneuvers, by controlling the wings and the flight muscles involved. These flight muscles also exhibit asymmetric motor patterns while turning [8]. As mentioned above the flexibility of the feedback control circuit, may also permit to understand complex parameters involved in moth flight control by acquiring EMG signals from the flight muscles involved and simultaneously detecting wing beat frequency. Closed-loop experiments can be performed by making use of these observed asymmetries, converting the time difference therein and detected wing beat frequency to the voltage values. The feedback control method presented here can be applied to the visual flight simulator described by Gray et al. [26] and address the limitation presented by using an abdomen position sensor [26]. This proposed approach in conjunction with multichannel neurophysiological recording can be very helpful to examine central neuronal activity that may be involved in the control of flight in a realistic environment [42].

5.3.2 Application using Radio-Telemetric concept

Kutsch [40] has highlighted the disadvantages resulting from the study of locust flight in tethered conditions under both open-loop and closed-loop conditions. The disadvantages involved in studying tethered flight have also been dealt with at length elsewhere. In brief it can be suggested that tethered flight may bar the insect from receipt of sufficient information regarding its position in 3D space. Integration of its position, velocity and acceleration and other parameters is required for the insect to move along a determined path. Kutsch suggests that mechanisms involved in the generation and control of flight motor output can be better understood by studying free or untethered flight of the insect. This requires us to deal with the complexities involved with the transfer/transmit and recording of muscle activity. Muscle activity data acquisition in an untethered flight may help us to understand the actual flight control under closed-loop conditions. Kutsch suggested the use of '*Radio-Telemetric Transmission'* of muscle activity. The telemetric device has been presented in [15]. The feedback control circuit presented here for detecting DA time difference, wing beat frequency and their conversion to voltage values enabling us to perform both open and closed-loop experiments can also be extended using the concept of *'Radio-Telemetric Transmission'*. Hardware 'RX-5 Pentusa' system and software provided by TDT Tech. Ltd, Florida, USA have been used for this thesis work. An interface to receive data from a transmitter fitted on the locust using the concept suggested by Kutsch can be procured, and the feedback control circuit designed by us can be used to perform open-loop and closed-loop experiments during free flight. This would enable us to detect DA time difference and wing beat frequency using the *'Radio-Telemetric Transmission'* approach in free flight. Alternatively, wireless electrodes can be used in conjunction with this

feedback control circuit to perform closed-loop experiments and investigate kinematics of locust flight.

5.4 Limitations

The feedback control circuit does exhibit the performance as expected; however certain limitations can be recognized. The circuit relies heavily on the DA time difference which in turn is a function of the spike time difference. To detect the potential spikes 'SortSpike2' [38] has been used. As described in Chapter 3, this component sorts/detects spikes i.e. identifies the firing of a motor neuron from the left and right wing based on threshold voltage setting performed in real-time. The threshold voltage setting was performed using 'sliders', which set the value of coefficients and the sort code for the 'SortSpike2' component. A manual error in setting the threshold too high or too low may lead to incorrect identification of spikes and thus result in incorrect DA time difference values. Incorrect DA time difference values may also result due to abnormal flight of the animal with wing beat frequency less than 10 Hz. This would require the user (investigator) to interrupt and change the threshold values.

Locusts may not always exhibit a steady flight and hence an intermittent flight coupled with intended bias towards right or left and low wing beat frequency may be observed. Such animals can be considered as *"bad fliers"* [7]. *"Bad fliers"* may exhibit abnormal motor output and hence may invite undesired interruption from the user to alter the threshold voltage levels for spike detection. The DA time difference thus obtained may not be considered as the actual DA time difference, as the flight was in itself not a steady flight. It can be suggested that the performance of the feedback control circuit is restricted to experiments related to tethered flight. Also, it can be argued that, the restriction of its body may have prevented it from moving freely, and in turn have insufficient information about its location and flight parameters like velocity

and acceleration in the flight simulator. Shoemaker and Robertson [28] were able to observe asymmetries in the timing of firing of m97 (forewing first basalar) muscles even in tethered flights and hence have suggested that tethering may not cause significant bias. This strengthens our claim that the voltage waveforms observed during the experiments did not display any effect of tether.

Placement of electrodes is very crucial for performing these experiments and obtaining better signals. An error in placement of electrodes may result in signals being recorded from a different set of muscles rather than from m97. Earlier, in this chapter it has been mentioned that we were not able to acquire good quality EMG signals (Figures 5.1 and 5.2). In spite of this drawback setting the correct value of threshold in real-time we were able to identify spikes. This suggests that the circuit was able to work as expected.

Some other factors that may affect EMG recordings can be the distance of the electrode from the muscle i.e. excessive long electrodes may get entangled in the insect's wings and create artifacts. The electrode material also plays an equally important role in obtaining good EMGs. For our experiments we did not encounter any problems pertaining to electrode material.

Use of EMG signals as a parameter for feedback control can also be considered as a limitation. Pearson and Wolf [16] have argued that EMG data analysis cannot be considered as an only approach to understand motor pattern generation for locust flight. Pearson and Wolf [16] have suggested that if the motor pattern is altered due to deafferentation (lack of sensory input from sense organs resulting from multiple reasons) the animal may account for it and the EMG activity observed may not appear to be significantly different. In such cases, using the feedback control circuit it is possible to detect spikes and obtain DA time difference values. However, occurrence of plasticity due to various reasons cannot be ruled out. In the event of occurrence of

plasticity necessary values of DA may be obtained and the animal may be able to control the ‘Cube’, but it may not be because of m97 depressor muscles; as the motor pattern control may have been taken over by other sets of muscles. It is not possible to comment whether owing to this limitation, the circuit’s performance was affected, as a larger sample size may be needed, which is beyond the scope of this thesis work. Manual spike sorting (sorting spikes using commercially available software(s) and calculating DA time difference) for all animals has not been done as it does not fall under the objectives of this thesis work.

CHAPTER 6

CONCLUSION

The locust flight motor pattern can be interpreted as a sample and hold circuit integrating sensory information and retaining characteristics of the immediate past. We observed that the feedback control circuit displayed a high level of fidelity as the tethered locust was able to determine the position of its body in the yaw plane according to the differences in the timing of spikes of depressor motor neurons of the left and right wings. It can be suggested that analysis of EMG signals from m97 muscles permits real-time interactive control. This is supported by the fact that locusts were able to control the orientation of the 'Cube' based on the DA / m97 spike time difference obtained from the DA. It can be suggested that EMG spike time difference detection and the voltage values arising from its conversion can be considered as adequate to control any other stimulus or external devices operating within the permissible voltage range of 0-5 V. The variation observed in the timing of the muscle pairs would allow the insect to explore and seek combinations of time shifts to produce the best steering response during the flight. The objective of converting DA time difference to voltage values was met successfully as results were obtained in both the open-loop and closed-loop environment. The time difference and voltage relationship can be thought of as a linear relationship in a given environment. The feedback circuit can be called a spike-detecting sensor that converts the spike time difference into voltage values.

The feedback control circuit in conjunction with implanted electrodes or wireless electrodes aided by high speed video analysis will help to further investigate the neuronal mechanisms of aerodynamic control and the cellular processes of mechanosensory integration. The system can be of great aid in understanding the functioning of insect nervous system when challenged with changes in wing kinematics and aerodynamics for steering, and gliding

operations. The results can be utilized to explore algorithms designed for robots or anti-collision devices [4,33,34].

The research findings suggest that insects, which are self powered and tiny in nature, do operate with highly efficient flight muscle actuators. The research work suggests that electromyogram technology or EMG spike time difference can be used as input for neuroelectric joysticks or keyboards and hence could give a thrust to development of new applications in flight control, space, and the video game industry. It is possible to control the flight of the locust by using a MEMS (micro electro - mechanical systems) based neuromuscular prosthetic system that would stimulate other flight muscles. The MEMS can be powered by a sensor utilizing this spike time difference converted to voltage values. The results presented here suggest that EMG and spike time difference approach can be used to replicate a traditional joystick to perform experiments in a flight simulator.

References:

[1] M. Heisenberg and R. Wolf, "On the fine structure of yaw torque in visual flight orientation of *Drosophila melanogaster*", *Journal of Comparative Physiology A: Neuroethology, Sensory, Neural, and Behavioral Physiology*, vol. 130, no. 2, pp. 113-130, 1979.

[2] P.S. Baker, "Flying locust visual responses in a radial wind tunnel", *Journal of Comparative Physiology A: Neuroethology, Sensory, Neural, and Behavioral Physiology*, vol. 131, no. 1, pp. 39-47, 1979.

[3] R. M. Robertson and D. N. Reye, "Wing Movements associated with collision avoidance manoeuvres during flight in the locust – *Locusta Migratoria*", *Journal of Experimental Biology*, vol. 163, pp. 231-258, 1992.

[4] M. Blanchard and Paul F.M.J Verschure, "Using a mobile robot to study locust collision avoidance responses", *International Journal of Neural Systems*, vol. 9, no. 5, pp. 405-410, 1999.

[5] D. Robert and C.H.F. Rowell, "Locust flight steering I", *Journal of Comparative Physiology A: Neuroethology, Sensory, Neural, and Behavioral Physiology*, vol. 171, Iss: 1, pp. 41-51, 1992.

[6] D. Robert and C.H.F. Rowell, "Locust flight steering II, Acoustic avoidance manoeuvres and associated head movements, compared with correctional steering", *Journal of Comparative Physiology A: Neuroethology, Sensory, Neural, and Behavioral Physiology*, vol. 171, Iss: 1, pp. 53-62, 1992.

[7] B. Möhl, "Short-term learning during flight control in *Locusta Migratoria*", *Journal of Comparative Physiology A: Neuroethology, Sensory, Neural, and Behavioral Physiology*, vol. 163, no. 6, pp. 803-812, 1988.

[8] A. E. Kammer and W. Nachtigall , "Changing Phase Relationships among Motor Units during Flight in a Saturniid Moth", *Journal of Comparative Physiology A: Neuroethology, Sensory, Neural, and Behavioral Physiology*, vol. 83, no. 1, pp. 17-24, 1973.

[9] R. M. Robertson and A. G. Johnson, "Collision avoidance of flying locusts: steering torques and behavior", *The Journal of Experimental Biology*, vol. 183, Iss: 4, pp. 35-60, 1993.

[10] D. Robert, "Visual steering under closed-loop conditions by flying locusts: flexibility of optomotor response and mechanisms of correctional steering", *Journal of Comparative Physiology A: Neuroethology, Sensory, Neural, and Behavioral Physiology*, vol. 164, no. 1, pp.15-24, January 1988.

[11] C.H.F. Rowell, "Mechanisms of flight steering in locusts", *Cellular and Molecular Life Sciences*, vol. 44, no. 5, pp. 389-395, May 1988.

[12] S. Berger and W. Kutsch, “Turning Manoeuvres in Free-Flying locusts: high-speed video monitoring”, *Journal of Experimental Zoology Part A: Comparative Experimental Biology*, vol. 299A, Iss: 2, pp. 127-138, 2003.

[13] J. W. Dawson, K. Dawson-Scully, D. Robert, and R. Meldrum Robertson, “Forewing asymmetries during auditory avoidance in flying locusts”, *Journal of Experimental Biology*, vol. 200, Iss: 17, pp. 2323-2335, 1997.

[14] R. M. Robertson, H. Xu, K. L. Shoemaker, and K. Dawson-Scully, “Exposure to Heat Shock Affects Thermosensitivity of the Locust Flight System”, *Journal of Neurobiology*, vol. 29, Iss: 3, pp. 367-383, 1996.

[15] W. Kutsch, G. Schwarz, H. Fischer, and H. Kautz, “Wireless Transmission of Muscle Potentials during Free Flight of a Locust”, *Journal of Experimental Biology*, vol. 185, Iss: 1, pp. 367-373, 1993.

[16] K. G. Pearson and H. Wolf, “Timing of forewing elevator activity during flight in the locust”, *Journal of Comparative Physiology A: Neuroethology, Sensory, Neural, and Behavioral Physiology*, vol. 165, no. 2, pp. 217-227, 1989.

[17] D. M. Wilson and T. Weis-Fogh, “Patterned activity of coordinated, motor units, studied in flying locusts”, *Journal of Experimental Biology*, vol. 39, pp. 643-668, 1962.

[18] Robert Elson and Hans Joachim Pflüger, “ The Activity of a steering muscle in flying locusts” *Journal of Experimental Biology*, vol. 120, pp. 421- 441, 1986.

[19] T. Weis Fogh, “Biology and Physics of Locust Flight. II. Flight Performance of the Desert Locust (*Schistocerca gregaria*)”, *Philosophical Transactions of the Royal Society of London. Series B, Biological Sciences*, vol. 239, no. 667, pp. 459-510, 1956.

[20] W. Reichardt and H. Wenking, “Optical Detection and Fixation of Objects by Fixed Flying Flies”, *Naturwissenschaften*, vol. 56, no. 8, page 424, 1969.

[21] J. M. Zanker, M. Egelhaaf, and Anne-Kathrin Warzecha, “On the coordination of motor output during visual flight control of flies”, *Journal of Comparative Physiology A: Neuroethology, Sensory, Neural, and Behavioral Physiology*, vol. 169, no. 2, pp. 127-134, 1991.

[22] B. Kimmerle, J. Eickermann, and M. Egelhaaf, “Object fixation by the blowfly during tethered flight in a simulated three-dimensional environment”, *Journal of Experimental Biology*, vol. 203, Iss: 11, pp. 1723-1732, 2000.

[23] C. N. Balint and M. H. Dickinson, “The correlation between wing kinematics and steering muscle activity in the blowfly *Calliphora vicin*”, *Journal of Experimental Biology*, vol. 204, pp. 4213-4226, 2001.

[24] K. G**.** Götz, Bewegungssehen and Flugsteuerung bei der Fliege *Drosophila*. In *BIONA-Report 2* (ed. W. Nachtigall), pp. 21-34. Stuttgart: Fischer. 1983.

[25] K. G**.** Götz, "Course control, metabolism and wing interference during ultralong tethered flight in *Drosophila melanogaster", Journal of Experimental Biology*, vol. 128, Iss: 1, pp. 35-46, 1987.

[26] J. R. Gray, V. Pawlowski, and M. A. Willis, "A method for recording behavior and multineuronal CNS activity from tethered insects flying in virtual space", *Journal of Neuroscience Methods*, vol. 120, Iss: 2, pp. 211-223. October 2002.

[27] B. Möhl and W. Zarnack, "Activity of the direct downstroke flight muscles of *Locusta migratoria* (*L*.) during steering behavior in flight. I. Patterns of time shift", *Journal of Comparative Physiology A: Neurophysiology, Sensory, Neural, and Behavioral Physiology*, vol. 118, pp: 215-233, 1977.

[28] K. L. Shoemaker and R. M. Robertson, "Flight motor patterns of locusts responding to thermal stimuli", *Journal of Comparative Physiology A: Neuroethology, Sensory, Neural, and Behavioral Physiology*, vol. 183, Iss: 4, pp. 477-488, October 1998.

[29] A. Arkles and J. R. Gray, "Real-time feedback of virtual stimuli for neuroethological research", unpublished (2006-2007).

[30] H. Cruse, J. Dean, and H. Ritte, *Prerational Intelligence: interdisciplinary perspectives on the behaviour of natural and artificial systems*, Springer, 2000.

[31] B. B. Guest and J. R**.** Gray, "Responses of a looming-sensitive neuron to compound and paired object approaches", *Journal of Neurophysioliology*, vol. 95, pp: 1428-1441, 2006.

[32] M. Burrows, *The Neurobiology of an Insect Brain*, New York: Oxford University Press, 1996.

[33] M. Blanchard, C. Rind, and Paul F.M.J Verschure, "How accurate need sensory coding be for behavior? Experiments using a mobile robot", *Neurocomputing*, vol. 38-40, pp. 1113-1119, 2001.

[34] S. Bermúdez i Badia, P. Pyk, and Paul F.M.J. Verschure, "A Biologically Based Flight Control System for a Blimp-based UAV", *Proceedings of the 2005 IEEE, International Conference on Robotics and Automation, Barcelona, Spain, April 2005*, pp. 3053-3059, 2005.

[35] Available: http://earthobservatory.nasa.gov/Study/Locusts/locusts3.html Accessed: September 2008.

[36] W. Kutsch, S. Berger, and H. Kautz, "Turning Manoeurvres in Free-flying locusts: Two-channel Radio-Telemetric Transmission of Muscle Activity", *Journal of Experimental Zoology Part A: Comparative Experimental Biology*, vol. 299A, Iss: 2, pp. 139-150, 2003.

[37] R. D. Santer, P. J. Simmons, and F. Claire Rind, “Gliding behaviour elicited by lateral looming stimuli in flying locusts”, *Journal of Comparative Physiology A: Neuroethology, Sensory, Neural, and Behavioral Physiology*, vol.191, no. 1, pp. 61-73, 2005.

[38] Tucker Davis Technologies, (online support help file) Available: http://www.tdt.com/Sys3WebHelp/TDTHelp.htm Accessed: Version 6.4, January 2007.

[39] R. M. Robertson and A. G. Johnson, “Retinal image size triggers obstacle avoidance during flight in locusts”, *Naturwissenschaften*, vol. 80, no. 4, pp. 176-178, 1993.

[40] W. Kutsch, “Telemetry in insects: the “intact animal approach””. *Theory in Biosciences*, vol. 118, pp. 29-53, 1999.

[41] R. Kern, C. Petereit, and M. Egelhaaf, “Neural processing of naturalistic optic flow”, *The Journal of Neuroscience*, vol. 21, pp. 1-5, 2001.

[42] D. M. Wolpert and Z. Ghahramani, “Computational principles of movement neuroscience”, *Nature Neuroscience Supplement*, vol. 3, pp. 1212-1217, 2000.

APPENDIX A
CIRCUIT DIAGRAMS

A.1 Basic trigger and timing control construct

This section contains the circuit diagram for the basic trigger and timing control construct. The circuit designed in the software was allocated to the main DSP.

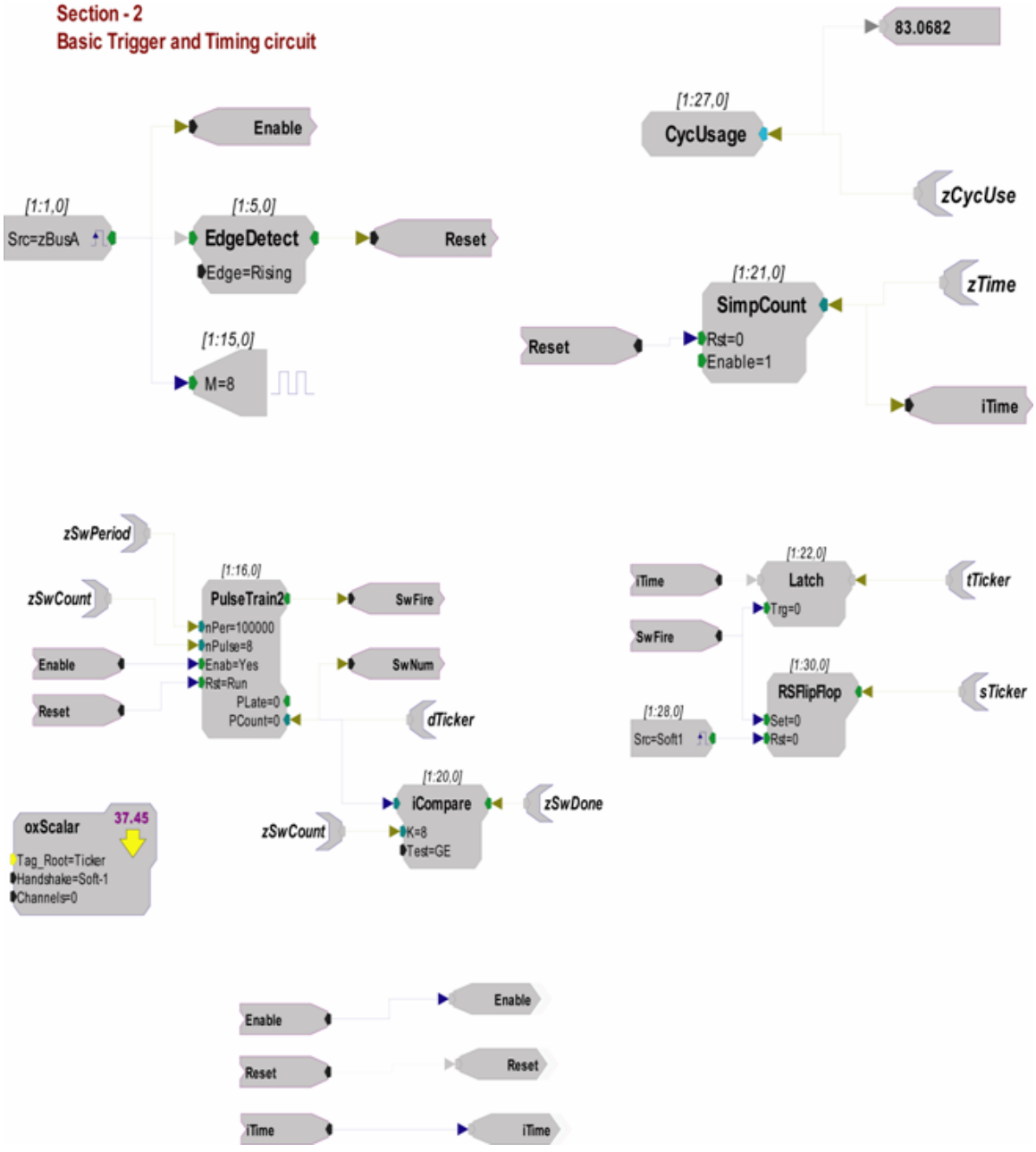

Figure A.1 Basic trigger and timing circuit allocated to main DSP.

The output of the ‘SimpCount’ (simple counter) was used to time stamp data via the ‘iTime’ line. Here the time value is measured in the number of samples from the instant the ‘Reset’ line went high and is automatically converted to seconds by ‘OpenWorkbench’ when time stamping data. The ‘CycUsage’ component was used to determine the processing power of the circuit. The cycle usage for the ‘SHARC’® DSPs used in the TDT system is dependent of sampling rate, processing power of the real time processor and total number of components in the circuit [38]. In our case, we used a sampling rate of 25 KHz. It was observed that the total cycle usage in our case never exceeded 17 %, which was significantly low as various signal processing tasks were distributed (signal processing tasks allocated to the main and other auxiliary DSPs), thus allowing us to have efficient recording. A parameter tag was used to access the ‘CycUsage’ output and view it in real time in ‘OpenController’ while the circuit was running. The parameter watch ‘ParWatch’[38] component connected to the ‘CycUsage’ displayed the cycle usage in ‘OpenController’ (refer Figure A.1) , thereby updating the user in real time.

Among the various other standard circuit control constructs available in the TDT software, the construct defining the number of acquisitions titled as ‘Basic Sweep Control’ [38] was modified and used. This sweep control construct marked the files with timing tick, typically set to 1 second via sweep period. Further details about the sweep control constructs can be obtained from the ‘OpenEx’ section of TDT’s online help manual [38].

The ‘zSwPeriod’ and the ‘zSwCount’ ‘parameter tags’ seen in figure A.1 were used to define the period and the number of sweeps. The ‘SwNum’ parameter tag pointed to the current sweep number. ‘SwNum’ displayed the value on the ‘Block Info’ sheet in ‘OpenWorkbench’ during run-time (when the circuit has been compiled and the code has been executed). During run-time the current sweep number would be compared to the total number of sweeps

('zSwCount') to determine when the sweep loop is complete. On this condition being satisfied, the output value is set high and the 'OpenWorkbench' would be flagged through the 'zSwDone' parameter tag to indicate that the last sweep had been reached.

Multiple 'zHopOut' and 'zHopIn' components [38] were used and renamed to represent 'Enable', 'Reset' and 'iTime'. 'RX5' being a multi-DSP system data transfer between multi-DSPs requires a central or main timing and control signal to acquire data, reset devices and perform other tasks [38]. 'Enable', and 'Reset' are thus produced by main DSP to activate, reset and perform other tasks as may be required by other DSPs. Apart from single channel transfer of signals, these components permitted the user to distribute processing tasks within a multi-DSP system like 'RX5'. The software requires the user to use 'zHopOut' and 'zHopIn' components in pairs.

APPENDIX B
CIRCUIT DIAGRAMS

B.1 Signal acquisition

This section contains the circuit diagram for the signal acquisition process and usage of multiplexers. The circuit designed in the software was allocated to the main DSP.

Section -3

Multiplexers have been used to switch between Fake Emg signals snd Real Signals.

Two Multiplexers have been used for 2 separate channels.

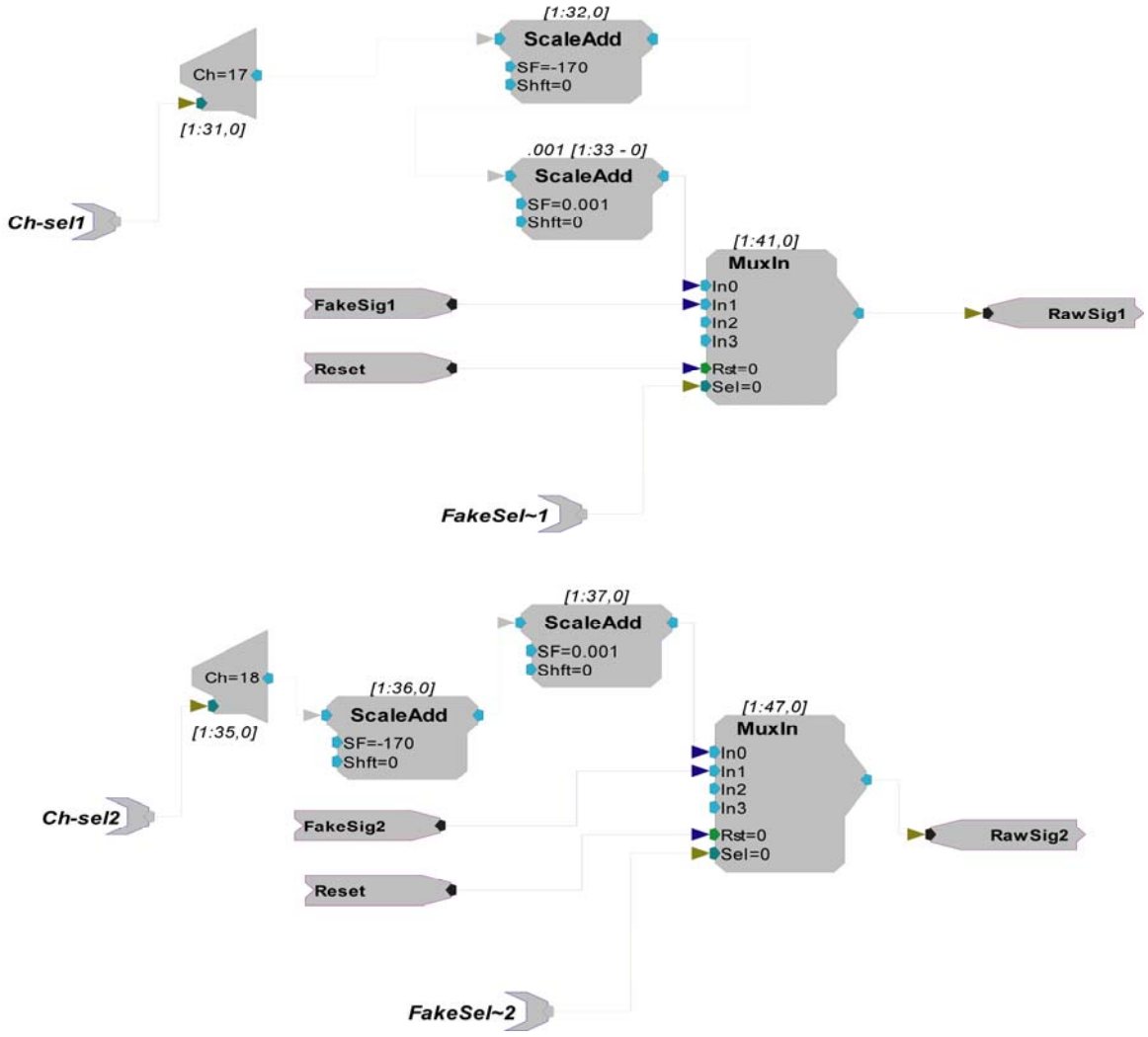

Figure B.1 Data-acquisition (signal acquisition). This figure represents page 2 in the software and provides details about the usage of multiplexer components, providing flexibility to select a signal from wave file and a live animal. For more detailed explanation refer text (Chapter 3, section 3.5).

APPENDIX C
CIRCUIT DIAGRAMS

C.1 EMG signal filtering

This section contains the circuit diagram for the EMG signal filtering. The circuit designed in the software was allocated to the main DSP.

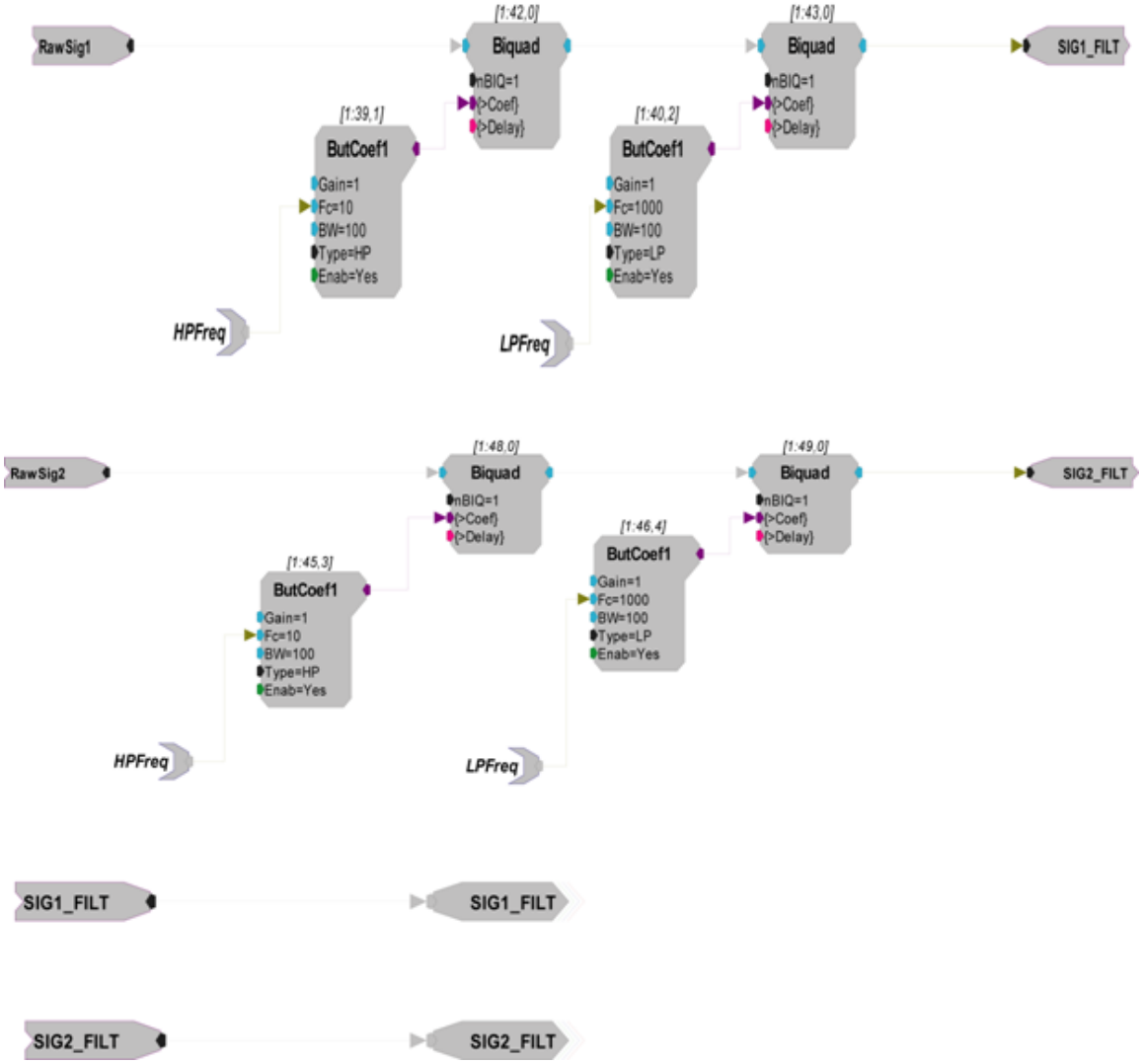

Figure C.1 EMG signal filtering. This figure represents page 3 in the software. This figure depicts the filtering process of the EMG signals from left and right wing. For more detailed explanation refer text (Chapter 3, section 3.5)

APPENDIX D
CIRCUIT DIAGRAMS

D.1 Spike detection on left EMG signals

This section presents the actual circuit diagrams (Figure D.1 - referred as page 5 in the software) pertaining to process of spike detection for EMGs from left EMGs and generation of time stamp T1. The process of spike detection on left wing EMGs was allocated to auxiliary DSPs I.

D.2 Spike detection on right EMG signals

This section presents the actual circuit diagrams (Figure D.2 - referred as page 6 in the software) pertaining to process of spike detection for EMGs from right wing and generation of time stamp T2. The process of spike detection on right wing EMGs was allocated to auxiliary DSP II.

D.3 Wing beat frequency detection and conversion to voltage

This section presents the actual circuit diagrams (Figure D.2 - referred as page 6 in the software) pertaining to process of wing beat frequency detection using ‘FindFreq’ component and its conversion to analog voltage values. Wing beat frequency detection was performed on right wing EMGs and the task was allocated to auxiliary DSP II.

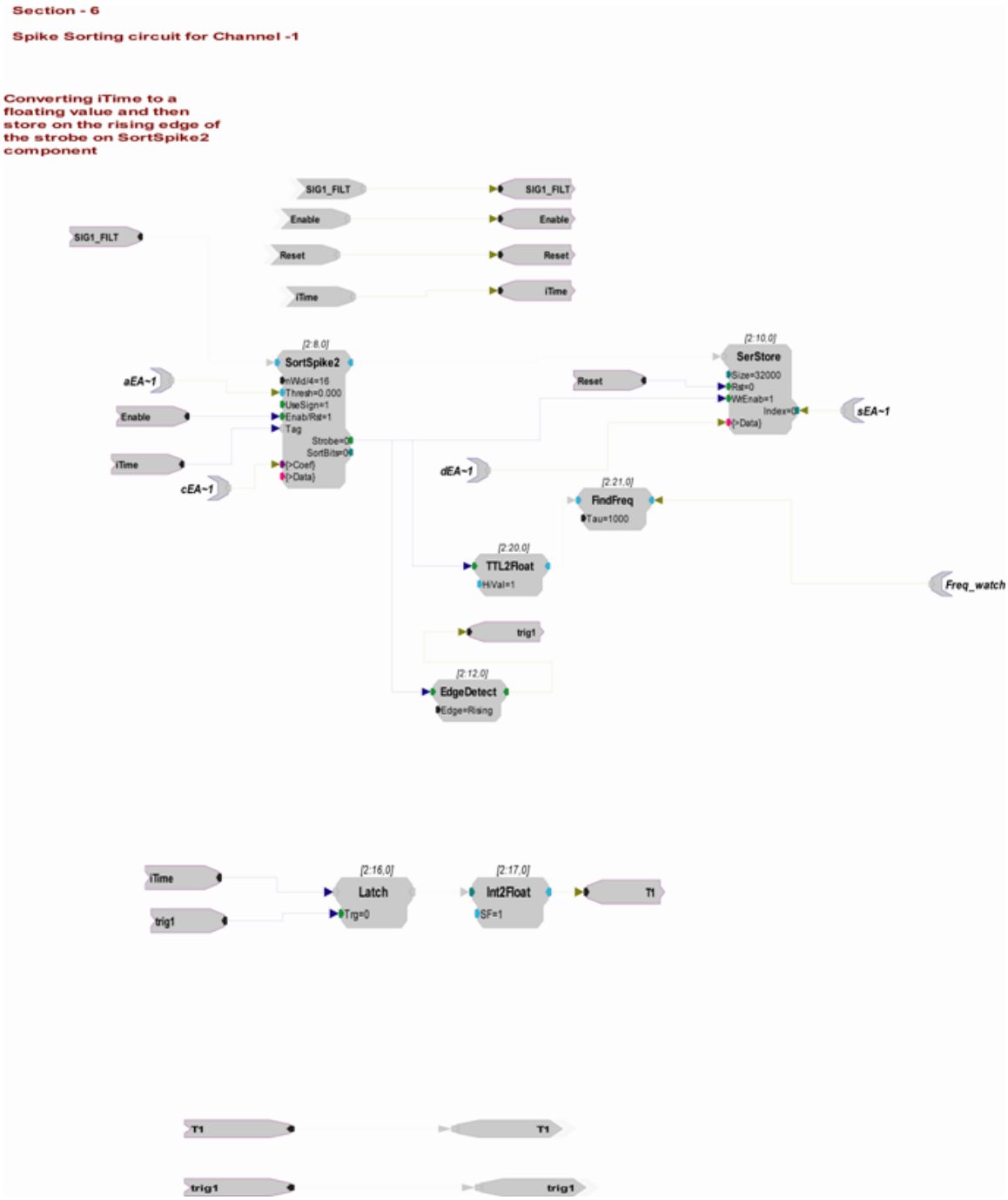

Figure D.1 Spike detection on Channel-1 Left EMG. This figure is a software representation (page 5 of the circuit) for the process of spike detection and generation of time stamp T1 on channel 1 (EMG signal from right wing). The detailed description of the spike detection process has been presented in text (Chapter3, Section 3.6). Tag root 'aEA~1' was connected to the 'Thresh' parameter to communicate the voltage threshold. The parameter tags, 'cEA~1' (corresponding to channel 1) would send the input received from the user via the sliders to the 'circuit' thus changing the sort codes values for 'SortSpike2', controlling and setting the coefficients determining time/voltage values in real-time.

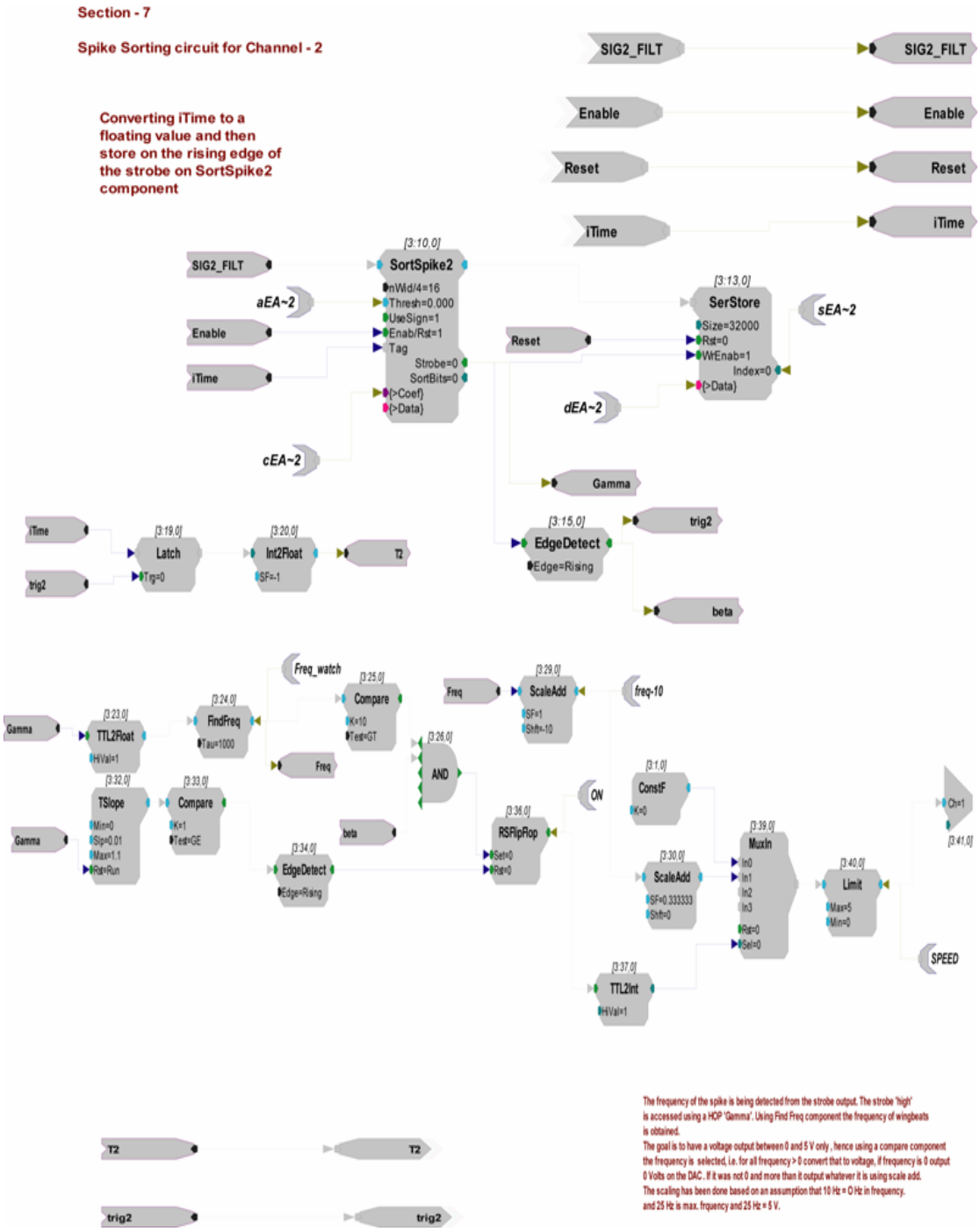

Figure D.2 Spike detection on Channel-2 Right EMG. This figure is a software representation (page 6 of the circuit) for the process of spike detection and generation of timestamp T2 on channel 2 (EMG signal from right wing). Tag root 'aEA~2' was connected to the 'Thresh' parameter to communicate the voltage threshold. The parameter tags, 'cEA~2' (corresponding to channel 2) would send the input received from the user via the sliders to the 'circuit' thus changing the sort codes values for 'SortSpike2', controlling and setting the coefficients determining time/voltage values in real-time. The detailed description for the above process has been presented in text (Chapter3, Section 3.6).

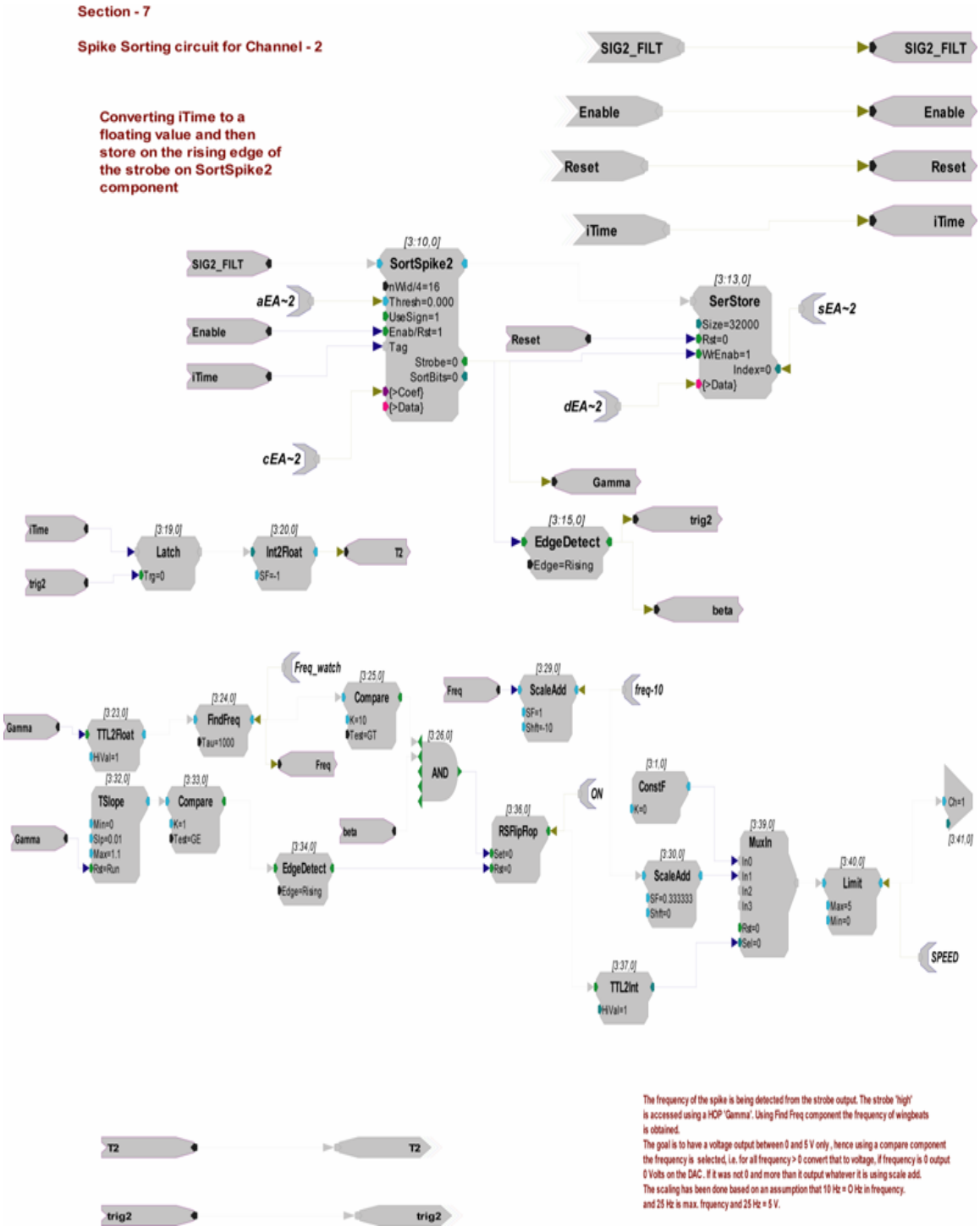

Figure D.3 wing beat frequency detection on Channel -2 Right EMG. This figure is a software representation (page 6 of the circuit) for the process of wing beat frequency detection using 'FindFreq' component and generation of analog voltage value 'V1'. The detailed description for the above process has been presented in text (Chapter3, Section 3.7). This figure is a reproduction of figure D.2

APPENDIX E
CIRCUIT DIAGRAMS

E.1 DA Time difference calculation and voltage conversion

This section presents the actual circuit diagram (Figure E.1 - referred as page 8 in the software) pertaining to calculation of DA time difference and its conversion to voltage. This task was allocated to DSP IV.

.

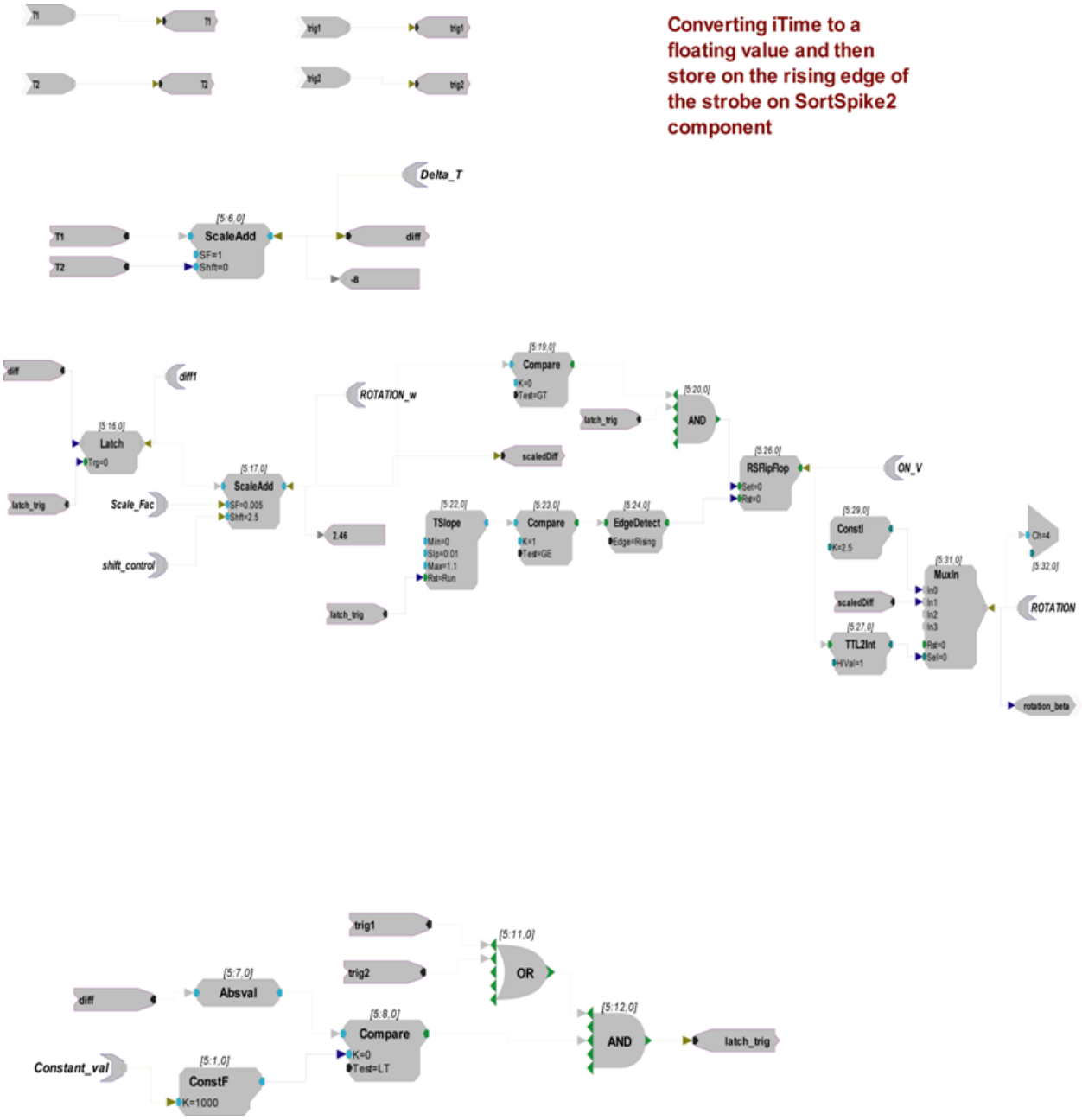

Figure E.1 Conversion of DA time difference into analog voltage values. This figure pertaining to conversion of DA time difference to analog voltage values ‘V2’ represents page 8 in the software. Detailed explaination of the process has been presented in text (refer Chapter 3, section 3.8).

APPENDIX F
DATA CONSTRUCTS

F.1 Data constructs for decimated data storage

The open and closed-loop experiments required control of timing during data acquisition, and spike detection events. For achieving these goals it was required to modify the 'circuit' constructs - group of components performing user defined tasks in 'OpenEx'. Due to mandatory software requirements it was necessary to have an associate header for data constructs when designing the circuits for 'OpenEx'[38]. These data constructs can be understood as group of components controlling the acquisition, management (processing and storage) of data. The 'circuit' headers within each data construct contained the required information for 'OpenWorkbench' to be able to acquire the data from the hardware and store it on the computer in a 'data tank' [38]. The information about the waveforms, data type, and the rate at which it would be received by 'OpenWorkbench' and stored in the 'data tank' on the computer; can only be obtained by using these headers [38]. The headers used for our design are the 'OxSnippet' and the 'OxStream'[38]. In our design the DSP-III was assigned these headers.

We have used the 'OxSnippet' based on the standard signal snippet data construct methods in TDT help manual [38]. The function of 'OxSnippet' is to store a spike event and sort code for each snippet [38]. As per the help manual [38], a 'circuit' designed to deal with continuous wave forms and store sorted spikes in data buffers needs to include 'OxSnippet' as 'circuit' header. With reference to our 'circuit' which has been designed to acquire EMG signals, detect spikes and store them in data buffers, the 'OxSnippet' header seemed to be a legitimate

choice for signal snippet ‘circuit’ constructs [38]. Recording of a continuous waveform required the usage of the ‘OxStream’ component [38].

Data constructs require a parameter tag to access the data [38]. The parameter tags ‘dPD~1’ and ‘dPD~2’ have been used for two channels of data associated with the data stream with tag root ‘PD’ for the ‘OxStream’ component. The tag root for the ‘OxSnippet’ component was set to ‘EA’. These ‘tag roots’ can be understood as a name that will be used by ‘OpenWorkbench’ to access the data, time stamps, and other information associated with these data construct[38]. The ‘sort code’ option for spike sorting was switched to the ‘Yes’ mode as we used ‘Sortspike2’ - spike acquisition component to generate a sort code for each snippet stored. The data format was set to ‘Float’.

The tag root for the ‘OxStream’ was set to PD. The block size (size of blocks in which the data would be acquired) was chosen abiding by the protocol described for ‘OxStream’ component in the help manual [38] which makes it mandatory for the user to have the block size value as an even number smaller enough to transfer data to the ‘data tank’ and reduce the cycle usage. For this design, block size was chosen as 32. The sort code option for spike sorting was switched to the ‘Yes’ mode. The data format was set to ‘Short’. The number of channels for both these data constructs was set to 2. As per software regulations and limitations of the ‘SortSpike2’ component, when the ‘OxStream’ component was to be used in conjunction with ‘PlotDec16’ and ‘Sortspike2’ components the decimation factor ‘Dec_Factor’ for ‘Oxstream’ should be set to half of the block size (‘nDec’) parameter of ‘PlotDec16’ component [38]. For this design the block size parameter of the ‘PlotDec16’ component was set to 256 and hence decimation factor ‘Dec_Factor’ for the ‘OxStream’ component for use with ‘PlotDec16’ was set to 128.

Page 7 (Figure F.1 appendix F) of the software refers to the standard ‘circuit’ for data reduction that has been modified for our use. Data reduction components were used to reduce memory allocation for storage on the computer. Since the open and closed-loop experiments relied on real-time data (real-time muscle activity and resulting spike(s)) rather than data stored using ‘PlotDec16’ component, it can be said that these data reduction components did not have impact on outcome of the experiment and spike data in general. Figure F.1 presents the actual circuit diagram page 7 of the feedback control ‘circuit’. The two ‘PlotDec16’ components receive the filtered EMGs from each channel, as input signals. The function of the component ‘PlotDec16’ is to track the max and min of the input for a set sample number (‘nDec’) [38], scale them and then output the values as the lower and upper portion of a word [38]. The advantages obtained by using the ‘PlotDec16’ component are beyond the scope of this thesis. The output from this component is a decimated value based on the components ‘SF’ (Scaling factor) [38] and block size (‘nDec’) [38]. These are then stored in the ‘SerStore’ (data buffers). For the ‘circuit’ in figure F.1 two channels of EMG signals have been associated with the ‘OxStream’ component through the use of the tag root ‘PD’ (Plot decimated). The ‘SIG1_FILT’ and ‘SIG2_FILT’ are the input channels (acquired EMG signal). The ‘Enable’ line from the ‘zTrigB’ initiates the plot decimation component (PlotDec16). A strobe signal is sent to ‘SerStore’ every 256 samples to store data.

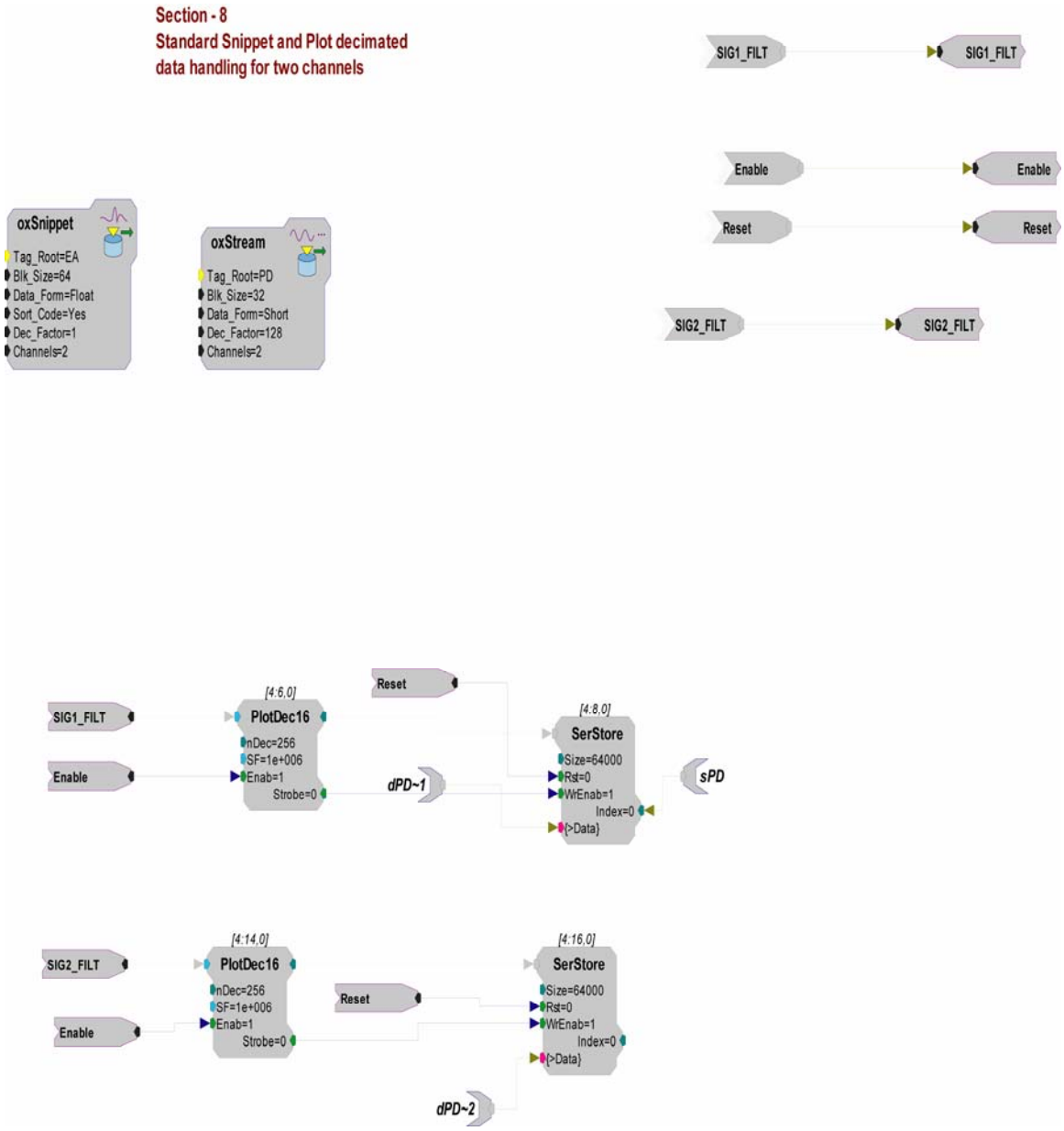

Figure F.1 Data constructs for storing detected spikes and decimated data. This figure represents page 7 of the feedback control in the software. The detailed description for the above process has been presented above.

F.2 Data Constructs for storing voltage and frequency values storage

Figure F.2 (refer next page) pertains to page 9 of the 'circuit' dealing with the constructs for storing the analog voltage values (DA converted to voltage) and storing the filtered EMGs for

reference. The reasons for using ‘OxStream’ as a ‘circuit’ header when recording continuous waveforms (EMGs) and the analog voltage values have been explained in earlier section. The tag root for ‘OxStream’ was set to ‘RAW’. The sort code option for spike sorting was switched to the ‘Yes’ mode. The data format was set to ‘Integer’. The number of channels was set to 3 as 3 continuous waveforms were being recorded and stored.

We have used ‘CompTo16D’ (compress to 16-bit) [38] component for data reduction and ‘SerStore’ for storing these waveforms. The reason for using ‘CompTo16D’ was to ensure that data was not stored when compression was not enabled. The ‘SIG1_FILT’ and ‘SIG2_FILT’ are the filtered EMG signals. The ‘Enable’ line connected to the ‘CompTo16D’ activates the component. In the ‘Enable’ mode the component would scale and convert a stream of 32-bit floating values to 16-bit fixed point numbers. Successive values would then be output in the upper and lower portions of a 32-bit integer [38]. Every 32 samples a strobe signal is sent to the ‘SerStore’ component to store the data. This reduction technique has been used to decrease memory allocation for data storage and double the data transfer rate to and from the computer [38]. Three ‘SerStore’ components have been used to store the filtered EMG signals- ‘SIG1_FILT’, ‘SIG2_FILT’ and the analog voltage value. The hop component ‘rotation beta’ carries the analog voltage value to the third ‘SerStore’ which is activated by the ‘Enable’ line. The parameter tags ‘dRAW~1’ , ‘dRAW~2’, and ‘dRAW~3’ with prefix ‘d’ for the tag root (indicating data) , are connected to the ‘Data’ pointer of the buffer indicating that data was being stored in the serial buffer. The parameter tag associated with a ‘Sync’ is identified by a ‘s’ prefix [38]. Following the software conventions the parameter tag ‘sRAW’ has been used only for one buffer to indicate the present position of the buffer [38].

This entire task was allocated to the auxiliary DSP – III.

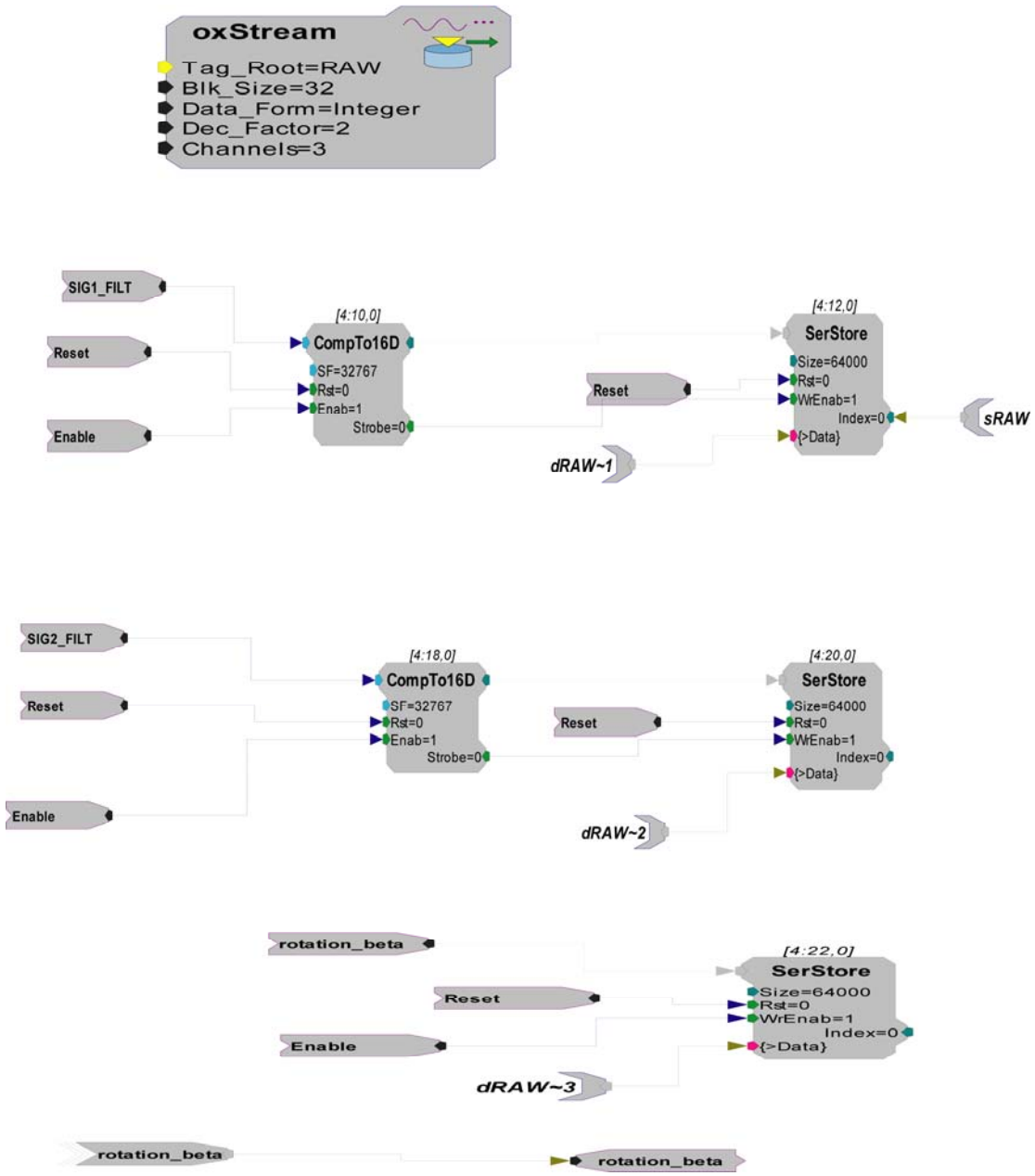

Figure F.2 Data constructs for storing voltage and frequency values. This figure represents page 9 of the feedback control in the software. The detailed description for the above process has been presented in text.